

The PTN-PTPRZ signal activates the  
AFAP1L2-dependent PI3K-AKT pathway for  
oligodendrocyte differentiation: Targeted  
inactivation of PTPRZ activity in mice

丹賀 直美

博士 (理学)

総合研究大学院大学

生命科学研究科

基礎生物学専攻

平成30 (2018) 年度

**The PTN-PTPRZ signal activates the AFAP1L2-dependent  
PI3K-AKT pathway for oligodendrocyte differentiation:  
Targeted inactivation of PTPRZ activity in mice**

Tanga, Naomi

SOKENDAI

(THE GRADUATE UNIVERSITY FOR ADVANCED STUDIES)

SCHOOL OF LIFE SCIENCE

DEPARTMENT OF BASIC BIOLOGY

A THESIS SUBMITTED FOR THE DEGREE OF  
DOCTOR OF PHILOSOPHY

## Table of Contents

<b>Abstract</b> .....	3
<b>Abbreviations</b> .....	6
<b>Chapter I. General introduction</b> .....	9
I. 1 Protein tyrosine phosphatase receptor type Z (PTPRZ) .....	10
I. 2 Binding molecules to the extracellular region of PTPRZ .....	11
I. 3 Substrates for PTPRZ .....	12
I. 4 Physiological functions of PTPRZ .....	13
I. 5 Role of PTPRZ in oligodendrocyte differentiation and myelination .....	14
I. 6 Outline of this thesis .....	15
<b>Chapter II. Identification of AFAP1L2 as PTPRZ substrate using OPC-like OL1 cells</b> ..	17
II. 1 Introduction .....	18
II. 2 Materials and methods .....	20
II. 3 Results .....	25
II. 4 Discussion .....	28
II. 5 Figures .....	31
<b>Chapter III. AFAP1L2 is the key substrate molecule coupling PTN-PTPRZ signal to the PI3K-AKT pathway and involved in oligodendrocyte differentiation</b> .....	39
III .1 Introduction .....	40
III. 2 Materials and methods .....	41
III.3 Results .....	44
III. 4 Discussion .....	46
III. 5 Figures .....	47
<b>Chapter IV. Generation and phenotype analyses of mice carrying the inactive phosphatase knock-in mutation of PTPRZ</b> .....	54
IV. 1 Introduction .....	55
IV. 2 Materials and methods .....	56
IV. 3 Results .....	60
IV. 4 Discussion .....	62
IV. 5 Figures .....	64
<b>Chapter V. Summary and conclusion</b> .....	73
V. 1 Discussion .....	74
V. 2 Figure .....	78
<b>References</b> .....	79
<b>Acknowledgements</b> .....	86

## **Abstract**

Myelination is an essential feature of the vertebrate nervous system that electrically insulates axons, thereby enabling the saltatory conduction of nerve impulses. Oligodendrocyte precursor cells (OPCs) are the principal source of myelinating oligodendrocytes. The protein tyrosine phosphorylation of various signaling molecules, which is reversibly regulated by Protein tyrosine kinases (PTKs) and protein tyrosine phosphatases (PTPs), is crucial for regulating OPC differentiation to oligodendrocytes. FYN plays essential roles in the induction of OPC differentiation by phosphorylating multiple distinct substrates including p190RhoGAP. Protein tyrosine phosphatase receptor type Z (PTPRZ) is one of the most abundant PTPs in OPCs. PTPRZ dephosphorylates p190 RhoGAP, thereby acting as a counterpart of FYN.

Three PTPRZ isoforms are generated by alternative splicing from a single gene: two transmembrane isoforms, PTPRZ-A and PTPRZ-B, and one secretory isoform, PTPRZ-S (or phosphacan). All isoforms are heavily modified with chondroitin sulfate chains, and identified as chondroitin sulfate proteoglycans (CSPGs) in the central nervous system. The chondroitin sulfate moiety on their extracellular domain of PTPRZ is essential for achieving high-affinity binding sites for the endogenous ligands such as pleiotrophin (PTN). It has been revealed that PTPRZ functions to maintain OPCs in an undifferentiated state. The inhibition of PTPase by its ligand pleiotrophin (PTN) promotes OPC differentiation; however, the substrate molecules of PTPRZ involved in the differentiation have not yet been elucidated in detail.

I herein demonstrated that the tyrosine phosphorylation of AFAP1L2, paxillin, ERBB4, GIT1, p190RhoGAP, and NYAP2 was enhanced in OPC-like OL1 my laboratory established cells by a treatment with PTN: OL1 cells are OPC-like cells established by my laboratory. Among them, AFAP1L2, an adaptor protein involved in the PI3K-AKT pathway, exhibited the strongest response to PTN. Therefore, I focused on AFAP1L2 in my study.

PTPRZ dephosphorylated AFAP1L2 at tyrosine residues *in vitro* and in HEK293T cells. Immunoprecipitation experiments showed that AFAP1L2 stably associated with the intracellular region of PTPRZ (Z-ICR). Because a public database search suggested fourteen potential tyrosine phosphorylation sites in AFAP1L2, I generated a series of AFAP1L2-F<sub>13</sub>-Y mutants, in which these tyrosine residues are replaced to phenylalanine residues except for one site. Co-immunoprecipitation experiments detected the binding of wild-type and F<sub>13</sub>-Y54 AFAP1L2 to p85 $\alpha$  of PI3K, indicating that Tyr-54 is the primary phosphorylation site for its association with p85 $\alpha$ . The co-transfection of wild-type PTPRZ-B, but not the catalytically-inactive Cys to Ser (CS) mutant, significantly reduced the tyrosine phosphorylation levels of the eleven mutants, in which AFAP1L2-F<sub>13</sub>-Y54 and -F<sub>13</sub>-Y56 showed the most prominent decreases.

In OL1 cells, the knockdown of AFAP1L2 or application of a PI3K inhibitor, LY294002 suppressed cell differentiation as well as the induced phosphorylation of AKT and mTOR induced by PTN. PTN also induced ERK1/2 phosphorylation and RhoA activation in OL1 cells, whereas LY294002 did not affect these responses, excluding the possibility of the non-specific actions of this

reagent. These results suggested that AFAP1L2-dependent PI3K-AKT-mTOR activation is one of the key downstream reactions of PTN-PTPRZ signaling during OPC differentiation.

My laboratory previously reported the earlier onset of the expression of myelin basic protein (MBP), a major protein of the myelin sheath, as well as the earlier initiation of myelination in neonatal brains in *Ptpz*-deficient (null) mice than in wild-type mice. To assess the physiological significance of its PTPase activity, I generated a *Ptpz* knock-in mouse harboring a catalytically-inactive CS mutation in its PTPase domain. The phosphorylation levels of AFAP1L2, AKT, and mTOR were higher, and the expression of oligodendrocyte markers, including MBP and myelin regulatory factor (MYRF), was stronger in CS knock-in brains than in wild-type brains on postnatal day 10; however, these differences mostly disappeared in the adult stage. Adult CS knock-in mice exhibited earlier remyelination after cuprizone-induced demyelination through the accelerated differentiation of OPCs. These phenotypes in CS knock-in mice were similar to those in *Ptpz*-deficient mice.

In summary, I revealed that the PTN-PTPRZ signal stimulates OPC differentiation partly by enhancing the tyrosine phosphorylation of AFAP1L2 to activate the PI3K-AKT pathway. PTN-induced PTPRZ inactivation regulates multiple signaling pathways, in cooperation with FYN kinase, as a hub molecule that is essential for oligodendrocyte differentiation and myelination.

## Abbreviations

AFAP1L2	actin filament-associated protein 1-like 2
bFGF	basic fibroblast growth factor
BrdU	5'-bromo-2-deoxyuridine
CAH	carbonic anhydrase-like domain
CBB	Coomassie brilliant blue
chABC	chondroitinase ABC
CNS	central nervous system
CSPG	chondroitin sulfate proteoglycan
DAPI	4', 6-diamidino-2-phenylindole
DMEM	Dulbecco's modified Eagle's medium
DTA	diphtheria toxin A
DTT	dithiothreitol
ERBB4	erb-b2 receptor tyrosine kinase 4
ERK	extracellular signal-regulated kinase
FBS	fetal bovine serum
FNIII	fibronectin type III domain
FRTL-5	Fischer Rat Thyroid cell line
Gapdh	Glyceraldehyde-3-phosphate dehydrogenase
GIT1	G protein-coupled receptor kinase interactor 1
HEK293T	Human embryonic kidney cells 293 T
HGF	Hepatocyte growth factor
HRP	horseradish peroxidase
IHC	immunohistochemical
IP	immunoprecipitation

MAGI1	membrane-associated guanylate kinase, WW and PDZ domain-containing 1
MAPK	mitogen-activated protein kinase
MBP	myelin basic protein
MEK	mitogen-activated protein kinase kinase
mTOR	The mammalian target of rapamycin
MYRF	myelin regulatory factor
N-CAM	neural cell adhesion molecule
Neo	neomycin
NG2	neural/glial antigen 2 chondroitin sulfate
NRG1	neureglin1
NYAP2	neuronal tyrosine-phosphorylated phosphoinositide-3-kinase adaptor 2
OPC	oligodendrocyte precursor cell
P	postnatal day
PBS	phosphate buffered saline
PDGF	platelet-derived growth factor
PI3K	phosphoinositide 3-kinase
PTN	pleiotrophin
PTK	protein tyrosine kinase
PTP	protein tyrosine phosphatase
PTPRZ	protein tyrosine phosphatase receptor type Z
PVDF	polyvinylidene fluoride
p85 $\alpha$	Phosphatidylinositol 3-kinase regulatory subunit alpha
RhoA	ras homolog family member A
RhoGAP	Rho GTPase-activating protein
ROCK	Rho-associated coiled-coil containing protein kinase
RT-PCR	reverse transcription PCR

SDS-PAGE	sodium dodecyl sulfate-polyacrylamide gel electrophoresis
SPF	specific pathogen-free
TBS	Tris-buffered saline
TH	thyroid hormone
TJP2	tight junction protein 2
TMB	tetramethylbenzidine
TrkA	Tropomyosin receptor kinase A
TUNEL	Terminal deoxyribonucleotidyl transferase-mediated dUTP-digoxigenin nick
end labeling	
UBR3	ubiquitin protein ligase E3 component n-recognin 3
U87MG	Uppsala 87 Malignant Glioma
WAVE1	Wiskott-Aldrich syndrome protein family member 1

# **Chapter I**

## **General introduction**

## **I. 1 Protein tyrosine phosphatase receptor type Z (PTPRZ)**

Protein tyrosine phosphorylation is one of the critical mechanism for signal transduction, and reversibly regulated by protein tyrosine kinases (PTKs) and protein tyrosine phosphatases (PTPs). Receptor-like PTPs (RPTPs) are a structurally and functionally diverse family of enzymes comprised of 8 subfamilies (Andersen et al., 2001). Most RPTPs have a structure composed of a unique extracellular domain, a single transmembrane domain, and either one or two intracellular catalytic PTP domains. In the latter case, the membrane proximal PTP domain (PTP-D1) exhibits PTP activity, whereas the distal PTP domain (PTP-D2) has negligible or no catalytic activity (Andersen et al., 2001).

Protein tyrosine phosphatase receptor type Z (PTPRZ, also called PTP $\zeta$ ) is a member of the R5 RPTP subfamily together with PTPRG (PTP $\gamma$ ). The D2 of PTPRG has been postulated to be essential for “head-to-toe” inactive dimer formation (Barr et al., 2009). PTPRZ and PTPRG structurally resemble each other and consist of a carbonic anhydrase (CAH)-like domain and fibronectin type III-like domain extracellularly, as well as two phosphatase domains intracellularly with a canonical PDZ-binding motif (-Ser-Leu-Val) located at their carboxyl terminal ends (Fujikawa et al., 2007b; Kawachi et al., 1999). However, their tissue distribution differs: PTPRG is ubiquitously, but PTPRZ is predominantly, expressed in the central nerves system (CNS).

Three isoform proteins of PTPRZ are generated by alternative splicing from a single Ptpz gene; the two transmembrane isoforms PTPRZ-A and PTPRZ-B and the secretory isoform PTPRZ-S corresponding to the extracellular portion of PTPRZ-A (also known as phosphacan or 6B4

proteoglycan), all of which are expressed as chondroitin sulfate proteoglycans in the brain (Canoll et al., 1996; Chow et al., 2008c; Nishiwaki et al., 1998, and references cited therein). PTPRZ-A and -B protein expression levels are down-regulated by metalloproteinase or plasmin-mediated digestion under physiological conditions (Chow et al., 2008a; Chow et al., 2008b). Therefore, the full-length PTPRZ-A protein is rarely observed in the adult mouse brain, and its resultant extracellular fragment ( $Z_A$ -ECF) is detected at the same molecular size as PTPRZ-S (Chow et al., 2008b). The receptor isoforms are now further subdivided into two submembers, “conventional PTPRZ-A or -B” and “exon 16-deleted PTPRZ- $A_{\Delta ex16}$  or  $-B_{\Delta ex16}$ ”, respectively (Fujikawa et al., 2017a). In this paper, I refer to both sets collectively as “PTPRZ-A or-B” for the reader's convenience.

## **I.2 Binding molecules to the extracellular region of PTPRZ**

It has been identified growth factors such as pleiotrophin (PTN)/heparin-binding growth-associated molecule (HB-GAM) (Fukada et al., 2006; Kawachi et al., 2001; Kuboyama et al., 2015; Maeda et al., 1996), midkine (MK) (Maeda et al., 1999), and interleukin-34 (IL-34) (Nandi et al., 2013) as inhibitory ligands for PTPRZ. The chondroitin sulfate moiety of PTPRZ is essential for achieving high-affinity binding sites for PTN, MK, and IL-34 (Maeda et al., 1999; Maeda et al., 1996; Nandi et al., 2013). PTN has been shown to inactivate the intracellular catalytic activity of PTPRZ-B by inducing molecular oligomerization in baby hamster kidney (BHK)-21 cells (Fukada et al., 2006). PTPRZ-S is one of the extracellular matrix (ECM) and perineuronal net molecules serving as a

substratum for multiple cell adhesion molecules including F3/contactin, N-CAM, or TAG1 (Xu et al., 2014).

### **I.3 Substrates for PTPRZ**

My laboratory previously reported a genetic method to screen for PTP substrates named the ‘yeast substrate-trapping system’ based on the yeast two-hybrid system with two modifications (Fukada et al., 2005; Kawachi et al., 2001): the conditional expression of a PTK to tyrosine-phosphorylate the prey protein, and screening using a substrate-trap PTP mutant as bait. Using this method, my laboratory has successfully identified several substrate candidates for PTPRZ, including G protein-coupled receptor kinase-interactor 1 (GIT1), GTPase-activating protein for Rho GTPase (p190RhoGAP), membrane-associated guanylate kinase, WW and PDZ domain-containing 1 (Magi1), and PDZ and coiled-coil motif containing (Gopc, also called PIST) (Fukada et al., 2006; Fukada et al., 2005; Kawachi et al., 2001). Afterwards, my laboratory has already proved that a number of molecules are indeed physiological substrate molecules for PTPRZ, including p190RhoGAP (Fukada et al., 2006; Kuboyama et al., 2012b; Tamura et al., 2006), G protein-coupled receptor kinase-interactor 1 (GIT1) (Fujikawa et al., 2011; Kawachi et al., 2001), paxillin (Fujikawa et al., 2011; Muramatsu et al., 2004), membrane-associated guanylate kinase, WW and PDZ domain-containing 1 (MAGI1) (Fukada et al., 2006), ERBB4 (Fujikawa et al., 2007a), and TrkA (Shintani and Noda, 2008). In addition, the motif for substrate specificity of Ptprz was determined by examining the contribution of respective amino acid side chains. The consensus motif of substrate

site for Ptprz thus identified is Glu/Asp-Glu/Asp-Glu/Asp-Xaa-Ile/Val-pTyr-Xaa (Xaa is not an acidic residue) (Fujikawa et al., 2011). This sequence is quite different from Glu/Asp-pTyr-pTyr-Arg/Lys identified for the substrate site of PTP1B (Myers et al., 2001). Although initially viewed as broad-specificity 'housekeeping' enzymes, PTPs are actually highly selective enzymes.

#### **I. 4 Physiological functions of PTPRZ**

*Ptprz*-null knockout (*Ptprz*-KO) mice lacking the expression of all three isoforms were established in our laboratory (Shintani et al., 1998). They are apparently healthy and show no obvious morphological abnormalities in the brain at the adult stage; however, various phenotypes were identified in this knockout mice afterward. *Ptprz*-KO mice exhibit the early onset of oligodendrocyte differentiation and myelination in the developing brain (Kuboyama et al., 2012a; Kuboyama et al., 2015; Kuboyama et al., 2016). They show a reduced disease severity in the experimental autoimmune encephalomyelitis model (Kuboyama et al., 2012b) and accelerated remyelination in the cuprizone model (Kuboyama et al., 2015; Kuboyama et al., 2016). Behavioral and neurological studies identified impairments in spatial and contextual learning and memory functions (Niisato et al., 2005; Tamura et al., 2006). In peripheral tissues, gastric mucosal cells express PTPRZ-B isoform, though at lower levels. *Ptprz*-KO mice are resistant to gastric ulceration caused by VacA, a cytotoxin secreted by *Helicobacter pylori* (Fujikawa et al., 2003).

## **I. 5 Role of PTPRZ in oligodendrocyte differentiation and myelination**

The myelination of axonal fibers provides electrical insulation to axons, which facilitates the transmission of nerve impulses, and functions to maintain long-term axonal integrity (Funfschilling et al., 2012; Griffiths et al., 1998; Lee et al., 2012). In the CNS, oligodendrocyte precursor cells (OPCs) are the principal source of oligodendrocytes for the formation of myelin sheaths during development and in the remyelination of demyelinated axons in adulthood (Buffo and Rossi, 2013). Previous studies reported that protein tyrosine phosphorylation is crucially involved in the signal transduction mechanism for OPC differentiation into mature oligodendrocytes and myelin formation. FYN tyrosine kinase, a SRC family PTK, plays the most important role for OPC differentiation and myelination (Kramer-Albers and White, 2011; Lu et al., 2005). FYN activation drives OPC differentiation by coordinately regulating several downstream pathways including the Rho-ROCK (Kramer-Albers and White, 2011), MEK-ERK (Colognato et al., 2004; Perez et al., 2013; Xie et al., 2016), and phosphoinositide 3-kinase (PI3K)-AKT (Colognato et al., 2004; Flores et al., 2008; Goebbels et al., 2010) pathways. Consequently, *Fyn*-deficient mice show hypomyelination in the brain (Cui et al., 2005; Umemori et al., 1999).

PTPRZ is the most abundant RPTP in OPCs (Ranjan and Hudson, 1996; Sim et al., 2006). PTPRZ dephosphorylates p190RhoGAP, thereby acting as a counterpart of FYN (Kuboyama et al., 2012b; Kuboyama et al., 2015). The amounts of myelin basic protein (MBP) and myelinated axons in the brain at postnatal day 10, when myelination occurs, are significantly higher in *Ptprz*-deficient mice than in wild-type animals, indicating a suppressive role for PTPRZ in oligodendrocyte

differentiation (Kuboyama et al., 2012b). Consistent with the earlier onset of CNS myelination, oligodendrocytes appear earlier in primary cultures from *Ptprz*-deficient mice than from wild-type mice (Kuboyama et al., 2012b).

My laboratory established an oligodendrocyte-lineage cell line, OL1, from a *p53*-knockout mouse brain (Kuboyama et al., 2015). Immature OL1 cells are OPC-like cells expressing neural/glial antigen 2 chondroitin sulfate (NG2) proteoglycan. They also express PTPRZ-A and PTPRZ-B as chondroitin sulfate proteoglycans; however, their expression decreases after differentiation into oligodendrocytes, although PTPRZ-B remains weakly detectable (Kuboyama et al., 2015). Immature OL1 cells treated with PTN show increased p190RhoGAP phosphorylation and significantly enhanced thyroid hormone (TH)- induced differentiation to oligodendrocytes (Kuboyama et al., 2015). It has been demonstrated that PTN enhanced TH-induced OPC differentiation in a primary culture of glial cells from wild-type mice, but not *Ptprz*-deficient mice, indicating that its effects are mediated by PTPRZ (Fujikawa and Noda, 2016; Kuboyama et al., 2015).

## **I.6 Outline of this thesis**

In order to completely elucidate the PTN-PTPRZ signaling mechanisms involved in OPC differentiation, I first examined the effects of a PTN stimulation on the tyrosine phosphorylation levels of substrates and substrate candidates using OL1 cells. In the cell-based assay, AFAP1L2 exhibited the greatest increase in tyrosine phosphorylation following the PTN treatment. AFAP1L2, an adaptor protein of 130 kDa, is associated with the p85 $\alpha$  subunit of PI3K through the phosphorylation

at Tyr-54, thereby activating the PI3K-AKT pathway without altering ERK1/2 phosphorylation (Lodyga et al., 2009; Yamanaka et al., 2012). I revealed that AFAP1L2 was one of the *bona fide* substrates for PTPRZ, and coupled the PTN-PTPRZ signal to the PI3K-AKT-mTOR pathway for OPC differentiation. I also verified the *in vivo* relevance of these results by generating knock-in mice carrying a catalytically inactive Cys to Ser mutation in the *Ptprz* gene.

## **Chapter II**

### **Identification of AFAP1L2 as PTPRZ substrate using OPC-like OL1 cells**

## II.1 Introduction

My laboratory has already identified a number of physiological substrate molecules for PTPRZ, including p190RhoGAP (Fukada et al., 2006; Kuboyama et al., 2012b; Tamura et al., 2006), G protein-coupled receptor kinase-interactor 1 (GIT1) (Fujikawa et al., 2011; Kawachi et al., 2001), paxillin (Fujikawa et al., 2011; Muramatsu et al., 2004), membrane-associated guanylate kinase, WW and PDZ domain-containing 1 (MAGI1) (Fukada et al., 2006), ERBB4 (Fujikawa et al., 2007a), and TrkA (Shintani and Noda, 2008). In these substrate molecules, the amino acid sequences of the typical dephosphorylation site by PTPRZ are conserved (Fujikawa et al., 2011). Consequently, other substrate candidates have been suggested by the previous database search (Fujikawa et al., 2011), such as actin filament-associated protein 1-like 2 (AFAP1L2/XB130), neuronal tyrosine-phosphorylated phosphoinositide-3-kinase adaptor 2 (NYAP2), ubiquitin protein ligase E3 component n-recognin 3 (UBR3), and tight junction protein 2 (TJP2/ZO-2).

To identify the downstream targets of the PTN-PTPRZ signal for OPC differentiation, I herein examined the effects of a PTN stimulation on the tyrosine phosphorylation of substrate candidates for PTPRZ using OL1 cells as an OPC model. Immature OL1 cells express full-length PTPRZ-A and short PTPRZ-B receptor isoforms to maintain the undifferentiated state, and their inhibitory ligand PTN releases the PTPRZ-mediated differentiation blockage; through inactivation of their phosphatase activities. PTN enhances TH-induced OL1 differentiation however, it does not induce OL1 (or OPC) differentiation by itself (Kuboyama et al., 2015). Under TH-induced differentiation

conditions, I treated OL1 cells for 1 hr with or without PTN and estimated increases in the tyrosine phosphorylation levels of the substrates and substrate candidates of PTPRZ.

I focused on AFAP1L2, an adaptor protein of 130 kDa, because it showed the most prominent increase in PTN-induced tyrosine phosphorylation. AFAP1L2 contains the amino acid sequence D-E-E-Y(54)-I-Y(56)-M in the N-terminal region, which is well matched to the substrate motif of PTPRZ (Fujikawa et al., 2011). The phosphorylation at Tyr-54 in the YxxM motif is involved in the association of AFAP1L2 with the p85 $\alpha$  of PI3K, which leads to the activation of PI3K-AKT signaling (Lodyga et al., 2009; Yamanaka et al., 2012). To examine the relationship between AFAP1L2 and PTPRZ, I investigated the effects of PTPRZ enzyme activity on tyrosine residues of AFAP1L2 *in vitro*, and co-expression experiments in HEK293T cell.

## II. 2 Materials and methods

### Primary antibodies.

Rabbit antibodies against phosphorylated Tyr-1105 of p190RhoGAP (anti-pY1105) (Tamura et al., 2006), Tyr-554 of GIT1 (anti-pY554) and polyclonal antibodies against the extracellular region of PTPRZ (anti-PTPRZ-S) (Fujikawa et al., 2011) were described previously. The commercially available antibodies used in the present study were as follows: anti-AFAP1L2 (Abcam, Cat# ab113718), anti-ERBB4 (Santa Cruz Biotechnology, Cat# sc-283), anti-pY416 of FYN (Cell Signaling Technology, Cat# 2101), anti-pY527 of FYN (Cell Signaling Technology, Cat# 2105S), anti-FYN (Cell Signaling Technology, Cat# 4023; Sigma-Aldrich, Cat# P2992 for immunoprecipitation), anti-GIT1 (BD Biosciences, Cat# 611396; Santa Cruz Biotechnology, Cat# sc-13961 for immunoprecipitation), anti-MAGI1 (Santa Cruz Biotechnology, Cat# sc-11523), anti-MAGI2 (Millipore, Cat# AB9878), anti-NYAP2 (Santa Cruz Biotechnology, Cat# sc-139514), anti-p190RhoGAP (BD Biosciences, Cat# 610150; Cell Signaling Technology, Cat# 12164 for immunoprecipitation), anti-pY118 paxillin (Cell Signaling Technology, Cat# 2541), anti-paxillin (BD Biosciences, Cat# 610051), anti-phosphotyrosine, PY20 (Abcam, Cat# ab16389), anti-RhoA (Cytoskeleton, Cat# ARH03), anti-TJP2 (Santa Cruz Biotechnology, Cat# sc-11448), anti-UBR3 (Santa Cruz Biotechnology, Cat# sc-244561), anti-GFP (MBL International, Cat# 598), anti-FLAG (Sigma-Aldrich, Cat# F7425; Sigma-Aldrich, Cat# F3165 for immunoprecipitation) and anti-MYC (Rockland, Cat# 600-401-381).

### **OL1 cell culture**

The preparation of mouse oligodendrocyte-lineage OL1 cells was described previously (Kuboyama et al., 2015). OL1 cells ( $2.0 \times 10^4$  cells) were cultured on a poly-*L*-ornithine-coated 3.5-cm plastic dish with “basal medium” containing knock-out DMEM/F12 supplemented with 1× GlutaMAX, 1× StemPro Neural Supplement, 20 µg/ml of basic fibroblast growth factor (bFGF; Wako Pure Chemical), and 10 µg/ml of PDGF-AA under a humidified chamber at 37°C with 5% CO<sub>2</sub>. Recombinant human PTN produced in yeast (Fukada et al., 2006) was used in the experiment.

### **Western blotting**

Protein samples, such as cell or tissue extracts, immunocomplexes precipitated with Protein G-Sepharose, and RhoA precipitated with Rhotekin beads were separated on a 5 to 20% gradient gel (cat# E-R520L, ATTO Bioscience & Technology) by SDS-PAGE, followed by semi-dry electroblotting onto a PVDF membrane (Immobilon-P, Millipore). After blocking with 4% non-fat dry milk and 0.1% Triton X-100 in TBS, the membranes were incubated overnight with the respective antibodies. Regarding the probing of tyrosine phosphorylated proteins, 1% BSA and 0.1% Triton X-100 in TBS were used as blocking solution, with which antibodies were diluted. The binding of these antibodies was visualized with respective secondary horseradish peroxidase (HRP)-conjugated antibodies (GE Healthcare) and a chemiluminescent substrate (Luminata forte western HRP substrate,

Millipore), and detected using a CCD video camera system (Ez-capture MG, ATTO Bioscience & Technology).

### **Mammalian expression plasmids**

The mammalian expression plasmids, pZeoPTP $\zeta$  for PTPRZ-B (Kawachi et al., 2001) and pZeoPTP $\zeta$ -CS for its phosphatase-inactive CS mutant (Fujikawa et al., 2011), were described previously. pCAG-EGFP-PtprzICR-WT, -CS, -DA, and -CS mutants for the expression of EGFP-fused PTPRZ-ICR proteins (the wild type and its mutants) were generated by an in-frame insertion of its corresponding cDNA into the pCAG vector (Niwa et al., 1991). The construct pFLAG-AFAP1L2 for FLAG-tagged AFAP1L2 was generated by inserting the full-length cDNA of mouse AFAP1L2 (GenBank accession no. NM\_001177797) into the pcDNA-FLAG vector (Fukada et al., 2006). pMyc-p85 $\alpha$  for the MYC-tagged p85 $\alpha$  construct was generated by inserting the full-length cDNA of mouse p85 $\alpha$  (phosphoinositide-3-kinase regulatory subunit 1, GenBank accession no. NM\_001077495) into the pcDNA vector. cDNAs were prepared by RT-PCR from mouse brain total RNA. The expression constructs for the AFAP1L2 mutant proteins were generated from its parent plasmids using a QuikChange Multisite-directed Mutagenesis kit (Stratagene).

### **v-src-HEK293T cell culture and DNA transfection**

v-src-HEK293T cells stably expressing v-Src were developed and maintained in our laboratory (Fujikawa et al., 2011). Cells ( $3 \times 10^5$  cells) were cultured on a 3.5-cm dish coated with rat tail collagen in Dulbecco's modified Eagle's medium (DMEM) (Thermo Fisher Scientific, Cat# 11995)

supplemented with 10% fetal bovine serum (FBS) (cat #171012, Nichirei Biosciences) in a humidified incubator at 37°C with 5% CO<sub>2</sub>. After an overnight cultivation, cells were transfected with 0.8 µg of a pZeoPTPζ, pZeoPTPζ-CS, or control pZeo vector, together with 0.07 µg pFLAG-AFAP1L2 using the standard calcium phosphate technique. After 6 hrs, medium was changed to fresh culture medium and further cultured for 48 hrs.

### **Protein extraction and chondroitinase (chABC) digestion**

Mouse brains or cultured cells were extracted with 1% Nonidet P-40 in TBS (10 mM Tris-HCl, pH 7.4, 150 mM NaCl) containing 1 mM vanadate, 10 mM NaF, and protease inhibitors (EDTA-free Complete, Roche Applied Science). Regarding the detection of PTPRZ proteins, brain extracts (10 µl) were mixed with an equal volume of 0.2 M Tris-HCl, 60 mM sodium acetate, and 10 mM EDTA, pH 7.5 with 250 micro-units of chABC (cat #C3667, Sigma-Aldrich) at 37°C for 1 hr.

### **Immunoprecipitation**

After precleaning the extracts with Protein G-Sepharose (GE Healthcare), samples were subjected to immunoprecipitation using a combination of antibodies and Protein G-Sepharose beads.

### ***In vitro* PTPase assay**

Recombinant human PTPRZ1 enzyme proteins (the whole intracellular region of human PTPRZ1) were prepared as previously described (Fujikawa et al., 2016; Fujikawa et al., 2017b). FLAG-tagged

AFAP1L2 proteins expressed in v-src-HEK293T cells were immunoprecipitated using anti-FLAG beads. The immunocomplex on beads was washed, and bound proteins were solubilized in assay buffer (50 mM Tris, 50 mM Bis-Tris, and 100 mM acetate, pH 6.5, containing 100 µg/ml BSA, 5 mM DTT, and 0.1% Tween 20) (Fujikawa et al., 2017a). The enzymatic reaction was initiated by adding appropriate amounts of recombinant PTP proteins with or without SCB4380, a PTPRZ inhibitor (Fujikawa et al., 2016), and incubating at 37 °C for 5 min. The reaction was terminated by rapid dilution and washing with ice-cold TBS containing 1 mM vanadate. The tyrosine phosphorylation of AFAP1L2 proteins was then analyzed by Western blotting.

### **Image and statistical analyses**

Quantitative image analyses were performed using Adobe Photoshop CS6 software (Adobe Photoshop). Statistical analyses were performed using IBM SPSS Statistics 25 software (SPSS).

### II. 3 Results

The PTN treatment increased the tyrosine phosphorylation of AFAP1L2, paxillin, ERBB4, GIT1, p190RhoGAP, and NYAP2 in a descending order; however, marked changes were not detected in MAGI1, TJP2, or MAGI2 (Figure II-1a). The tyrosine phosphorylation of UBR3 was not detectable by Western blotting. Among the molecules that showed elevated tyrosine phosphorylation, paxillin (Fujikawa et al., 2011), ERBB4 (Fujikawa et al., 2007a), GIT1 (Fujikawa et al., 2011; Kawachi et al., 2001), and p190RhoGAP (Tamura et al., 2006) have already been verified as physiological PTPRZ substrates. The tyrosine phosphorylation of p190RhoGAP in OPCs was previously shown to be regulated by FYN (Liang et al., 2004) and PTPRZ (Kuboyama et al., 2012b) and the activity of Fyn is also shown to be regulated by tyrosine phosphorylation. However, PTN did not affect the tyrosine phosphorylation of FYN (Figure II-1a, two lanes at the bottom). Changes in the overall tyrosine phosphorylation pattern in cellular proteins were not detected (Figure II-1b). Taken together with the finding that the PTN-induced enhancement of OPC differentiation was not observed in *Ptprz*-deficient primary glial cells (Kuboyama et al., 2015), these results supported PTN-induced increases in the phosphorylation of these proteins being due to the inactivation of PTPRZ, but not the activation of FYN.

When AFAP1L2 was exogenously expressed in HEK293T cells with constitutively active v-Src, AFAP1L2 proteins were strongly tyrosine-phosphorylated (Figure II-2a,b). The tyrosine phosphorylation levels of AFAP1L2 following the co-expression of wild-type PTPRZ-B were lower

than in mock- or CS (PTP-inactive) mutant-transfected cells (Figure II-2a,b). *In vitro* experiments revealed that recombinant PTPRZ enzyme proteins efficiently dephosphorylated AFAP1L2 proteins, and this dephosphorylation was inhibited by the selective PTPRZ inhibitor, SCB4380 (Figure II-2c).

I also investigated the interaction between the entire intracellular region of PTPRZ (Z-ICR) and AFAP1L2 by co-immunoprecipitation. v-src-HEK293T cells were co-transfected with FLAG-tagged AFAP1L2 and green fluorescent protein (EGFP)-fused Z-ICR. Anti-FLAG immunoprecipitation showed that AFAP1L2 stably associated with wild-type Z-ICR (Figure II-3), suggesting recognition mechanism between AFAP1L2 and the ICR of PTPRZ. However, the DA substrate-trapping mutant of Z-ICR (Kawachi et al., 2001) exhibited a significantly higher binding ability than the wild type, suggesting that PTPRZ recognizes AFAP1L2 as a substrate through phospho-Tyr recognition in the substrate protein by the catalytic domain. Regarding the latter, PTPRZ is known to associate with PDZ domain-containing proteins, including MAGI1/3 and PSD95, through the C-terminal PDZ-binding motif in PTPRZ (Fujikawa et al., 2011). However, the PDZ-binding-motif mutant (SA mutant) of PTPRZ showed no significant difference in its association with AFAP1L2 (Figure II-3).

A public database search (PhosphoSitePlus) (Hornbeck et al., 2015) suggested that AFAP1L2 contains fourteen potential tyrosine phosphorylation sites (see Figure II-4a). I transfected v-src HEK293T cells with an expression plasmid for FLAG-tagged AFAP1L2-F<sub>14</sub>, in which all fourteen tyrosine residues were replaced with phenylalanine residues, and found that this replacement expectedly resulted in the complete disappearance of tyrosine phosphorylation (compare “F<sub>14</sub>” with

“*WT*” in Figure II-4b). Next, I generated a series of AFAP1L2-F<sub>13</sub>-Y mutants, in which individual phenylalanine residues were reconverted to tyrosine residues. Experiments to assess phosphorylation and dephosphorylation at each site using these AFAP1L2 mutants showed that phosphorylation occurred at thirteen sites other than Tyr-673 in v-src HEK293T cells (Figure II-4b). Co-immunoprecipitation experiments detected the binding of wild-type and F<sub>13</sub>-Y54 AFAP1L2 to MYC-tagged p85 $\alpha$  of PI3K, indicating that Tyr-54 is the primary phosphorylation site for its association with p85 $\alpha$  (Figure II-4c). The co-transfection of wild-type PTPRZ-B, but not the CS mutant, significantly reduced the tyrosine phosphorylation levels of the eleven mutants, in which AFAP1L2-F<sub>13</sub>-Y54 and -F<sub>13</sub>-Y56 showed the most prominent decreases (Figure II-4d). Consistently, recombinant PTPRZ proteins more efficiently dephosphorylated AFAP1L2-F<sub>13</sub>-Y54 than AFAP1L2-F<sub>13</sub>-Y383 *in vitro* (Figure II-5), indicating that the SH2 domain-binding motif was indeed the major dephosphorylation site of PTPRZ.

## II. 4 Discussion

The results obtained demonstrated that PTN increased tyrosine phosphorylation levels in AFAP1L2, paxillin, ERBB4, GIT1, and NYAP2 as well as p190RhoGAP (Kuboyama et al., 2012b; Kuboyama et al., 2015; Kuboyama et al., 2016). Among these, AFAP1L2 showed the most prominent increase in tyrosine phosphorylation upon the PTN treatment.

FYN plays essential roles in the induction of OPC differentiation by phosphorylating multiple distinct substrates including p190RhoGAP (Kramer-Albers and White, 2011). PTN-PTPRZ signaling may modulate the activity of a set of downstream targets of the FYN-regulated signaling pathways. My laboratory recently reported that PTN-induced PTPRZ inactivation enhanced the tyrosine phosphorylation levels of p190RhoGAP in OL1 cells and promoted the differentiation of OL1 cells (Kuboyama et al., 2015). The tyrosine phosphorylation of p190RhoGAP enhances GAP activity, thereby suppressing the Rho-ROCK pathway involved in the control of process formation in oligodendrocytes (Kramer-Albers and White, 2011; Liang et al., 2004). The expression of dominant-negative RhoA induced the extension of oligodendrocyte processes, whereas the introduction of constitutively-active RhoA hindered process formation in rat primary cultured OPCs (Liang et al., 2004), indicating that the FYN-p190RhoGAP-Rho-ROCK pathway controls morphological changes in mature oligodendrocytes. PTPRZ dephosphorylates p190RhoGAP as a counterpart of FYN without affecting the tyrosine phosphorylation of FYN itself (Kuboyama et al., 2012b) (Figure II-1).

PTPRZ preferentially dephosphorylates phosphotyrosine in the consensus motif sequence, E/D-E/D-E/D-X-I/V-pY-X (X is not an acidic residue), in physiologically relevant substrates, such as p190RhoGAP at Tyr-1105, paxillin at Tyr-118, GIT1 at Tyr-554, and MAGI1 at Tyr-373 (Fujikawa et al., 2011). Here, I identified AFAP1L2 as another substrate of PTPRZ which may be involved in the regulation of OPC differentiation. AFAP1L2 was efficiently dephosphorylated by PTPRZ and the two proteins co-immunoprecipitated, indicating that AFAP1L2 is a native substrate for PTPRZ. I identified phosphorylated Tyr-54 in AFAP1L2 as the primary site for p85 $\alpha$  binding, and demonstrated that PTPRZ efficiently dephosphorylated AFAP1L2, particularly at Tyr-54 and Tyr-56. It would be important to note that AFAP1L2 was recently identified among the top 50 oligodendrocyte-specific proteins (Sharma et al., 2015).

The effect of PTN on PTPRZ (peaking at 30 to 60 min) (Fukada et al., 2006) is considerably slower than that of EGF (epidermal growth factor) or PDGF (platelet-derived growth factor) on their receptor tyrosine kinases and their substrate molecules (usually peaks at ~ 5 min). The extracellular portion of PTPRZ is highly modified with negatively-charged chondroitin sulfate chains which prevent PTPRZ from spontaneous clustering (Kuboyama et al., 2016). The number of chondroitin sulfate chains attached to 6B4 proteoglycan (another name of PTPRZ-S secretory isoform of which structure corresponds to the extracellular portion of PTPRZ-A) was estimated to be 24 chains per core protein molecule (Maeda et al., 1995). Mouse PTPRZ-A and -S contain 31 potential chondroitin sulfate attachment sites (Ser-Gly or Gly-Ser) within the extracellular region. Based on simple calculations, the short receptor PTPRZ-B containing 13 potential sites is expected to be modified with

10 chondroitin sulfate chains per molecule. Accumulated binding of positively-charged PTN gradually neutralizes electrostatic repulsion between chondroitin sulfate chains, thereby inducing clustering of PTPRZ receptor isoforms, which leads to the inactivation of its intrinsic PTPase as the next step (Kuboyama et al., 2016). This appears to be a reason for the slower response to PTN. In my experience, it is difficult to detect the ligand effect of PTN on PTPRZ in some of the commonly used cell lines including HEK293T. I think that this may be due to a distinct sugar modification profile from that in OPCs: The chondroitin sulfate modification of PTPRZ-B is markedly weak in HEK293T (Chow et al., 2008b). The high affinity binding of positively-charged ligands to PTPRZ depends on chondroitin sulfate chains (Maeda et al., 1999; Maeda et al., 1996), and their sulfation patterns: Binding affinity of PTN is strong for chondroitin sulfate-E/D, moderate for chondroitin sulfate-C, and very weak for chondroitin sulfate-A (Maeda et al., 2003).

## II. 5 Figures

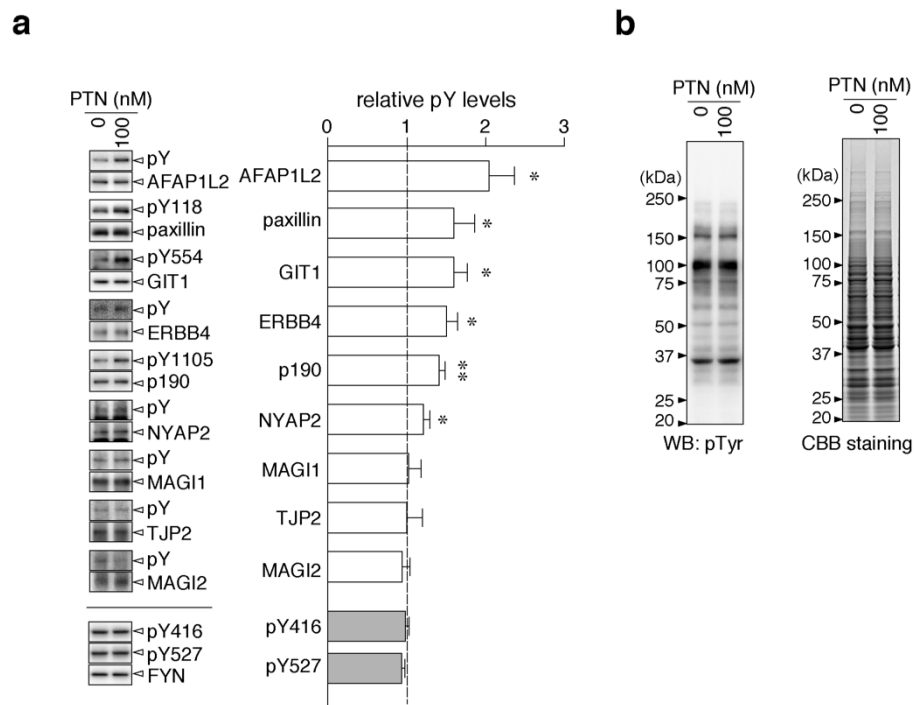


**Figure II-1 PTN-induced tyrosine phosphorylation in substrate candidates for PTPRZ in OL1**

**cells.** (a) Tyrosine phosphorylation levels in substrates and substrate candidates for PTPRZ. OL1 cells were treated with or without PTN for 1 hr. Cell extracts were immunoprecipitated with each respective antibody, and then subjected to Western blotting analyses. The phosphorylation of paxillin (Tyr-118), GIT1 (Tyr-554), p190 (Tyr-1105), and FYN (Tyr-416 and Tyr-527) was analyzed using the respective phosphorylation site-specific antibodies. Other data were obtained using a monoclonal antibody against phosphotyrosine (PY20). The bar plot on the right side shows phosphorylation levels as arbitrary densitometric units relative to those of the non-treated group. Data are the mean  $\pm$  S.E. (*error bars*) of three to six independent experiments. \*,  $p < 0.05$ ; \*\*,  $p < 0.01$ , significantly different from the non-treated control group by Welch's *t*-test. (b) Overall

tyrosine phosphorylation of total cellular proteins. The *left* panel shows the overall tyrosine phosphorylation pattern of OL1 cell extracts analyzed using PY20, and the *right* shows Coomassie Brilliant Blue (CBB) staining to verify the applied protein amounts.

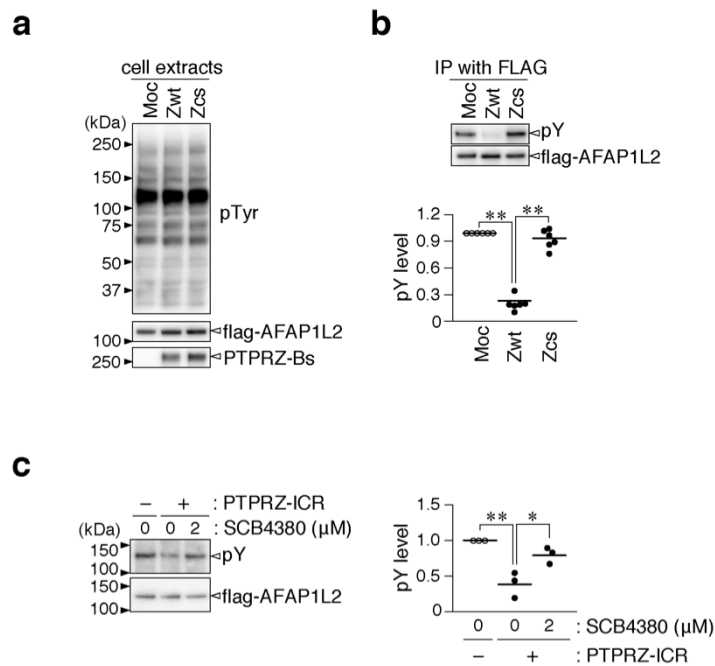


**Figure II-2 Dephosphorylation of AFAP1L2 by PTPRZ in cells.** (a) Overall tyrosine phosphorylation of cellular proteins and the expression of proteins. An expression construct for FLAG-tagged AFAP1L2 was transfected into  $\nu$ -Src-HEK293T cells (Fujikawa et al., 2011) together with wild-type PTPRZ-B ( $Z_{WT}$ ), its PTP-inactive Cys-1934 to Ser mutant ( $Z_{CS}$ ), or control vector ( $Moc$ ). After 48 hrs, cells were incubated in serum-free medium for 3 hrs. Cell extracts were examined using PY20, rabbit anti-PTPRZ-S (for PTPRZ-B proteins), and anti-FLAG (for flag-AFAP1L2 proteins). (b) Tyrosine phosphorylation levels of AFAP1L2. FLAG-tagged AFAP1L2 proteins immunoprecipitated from cell extracts using the anti-FLAG antibody were analyzed using PY20 and anti-AFAP1L2 antibodies. The scatter plot shows the signal intensity of PY20 staining relative to the moc control, in which each circle corresponds to an independent cell culture ( $n = 6$ ).

\*\* ,  $p < 0.01$ , significant difference between the indicated groups using a one-way analysis of variance (ANOVA) with Bonferroni's post hoc tests. (c) *In vitro* dephosphorylation of AFAP1L2 by PTPRZ. FLAG-tagged AFAP1L2 proteins purified by immunoprecipitation with anti-FLAG beads were incubated with human PTPRZ-ICR proteins in the presence or absence of SCB4380. Tyrosine phosphorylation levels were examined by Western blotting using PY20 and anti-AFAP1L2 antibodies. The scatter plot shows the signal intensity of PY20 staining relative to the non-treated control, in which each circle corresponds to an independent assay ( $n = 3$ ). \*,  $p < 0.05$ ; \*\*,  $p < 0.01$ , significant difference between the indicated groups using a one-way analysis of variance (ANOVA) with Bonferroni's post hoc tests.

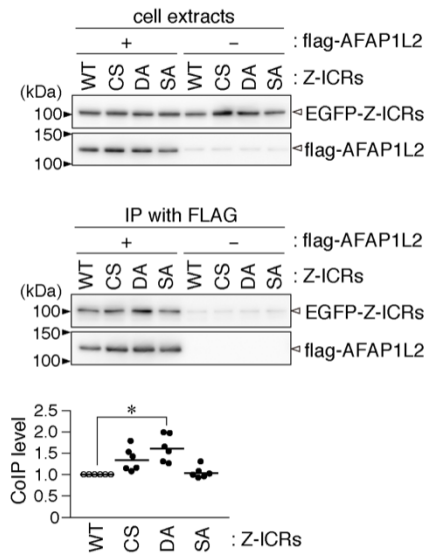


**Figure II-3 Co-immunoprecipitation experiments of AFAP1L2 and PTPRZ in cells.** EGFP-fused wild-type PTPRZ-ICR (*WT*), its CS, or Asp-1902 to Ala (DA), or Ser-2314 to Ala (SA) mutant was expressed in  $\nu$ -Src-HEK293T cells with or without FLAG-tagged AFAP1L2. Cell extracts were subjected to immunoprecipitation with an anti-FLAG antibody, and analyzed by Western blotting using anti-GFP and anti-FLAG antibodies. The scatter plot shows the signal intensity of anti-GFP staining, in which each circle corresponds to an independent cell culture ( $n = 6$ ). \*,  $p < 0.01$ , significant difference between the indicated groups using a one-way ANOVA analysis of variance with Bonferroni's post hoc tests.

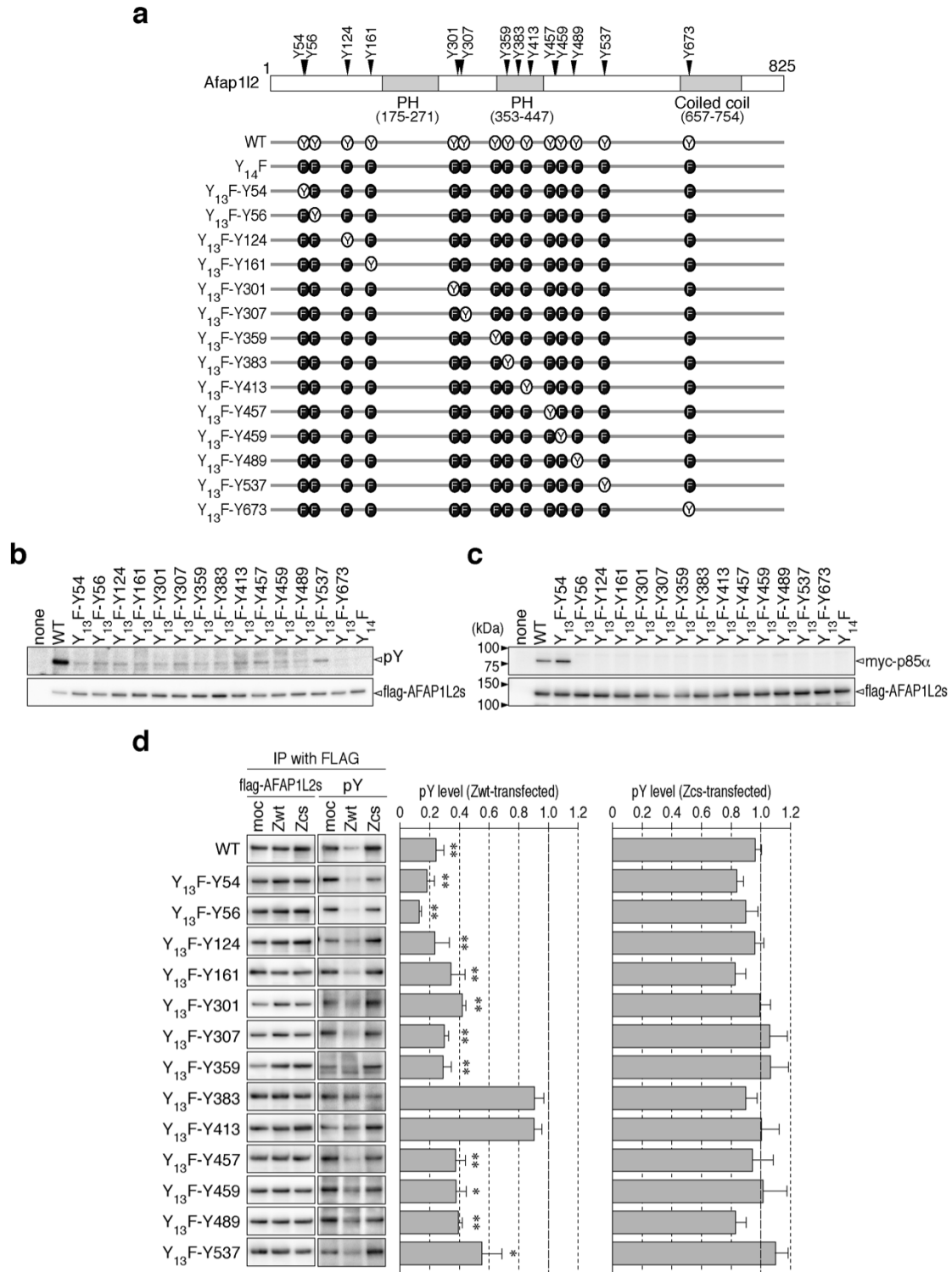


**Figure II-4 Identification of tyrosine phosphorylation sites in AFAP1L2 and their dephosphorylation by PTPRZ.** (a) Schematic representation of AFAP1L2 and the mutant constructs. Numbers correspond to amino acid residues of mouse AFAP1L2. PH, Pleckstrin-

homology domains. **(b)** Tyrosine phosphorylation of AFAP1L2 mutants. Expression constructs for FLAG-tagged wild-type AFAP1L2 or its mutants were transfected into  $\nu$ -Src-HEK293T, and their tyrosine phosphorylation levels were analyzed, as shown in Figure II-2b. The blots shown are a representative of two independent experiments with similar results. **(c)** Co-immunoprecipitation experiments. FLAG-tagged AFAP1L2 or its mutants were expressed in  $\nu$ -Src-HEK293T cells with MYC-tagged p85 $\alpha$ . Cell extracts were subjected to immunoprecipitation with an anti-FLAG antibody, and analyzed by Western blotting using anti-AFAP1L2 and anti-MYC antibodies. The blots shown are a representative of two independent experiments with similar results. **(d)** Dephosphorylation of AFAP1L2 mutants by PTPRZ. FLAG-tagged AFAP1L2 or its mutants were transfected together with the wild-type or CS PTPRZ-B, or control vector. The tyrosine phosphorylation of AFAP1L2 proteins was analyzed as above. The bar plot on the right side shows the signal intensity of PY20 staining relative to the moc control. Data are the mean  $\pm$  S.E. (*error bars*) of three independent experiments. \*,  $p < 0.05$ ; \*\*,  $p < 0.01$ , significantly different from the moc control in each group using a one-way ANOVA with Bonferroni's post hoc tests.

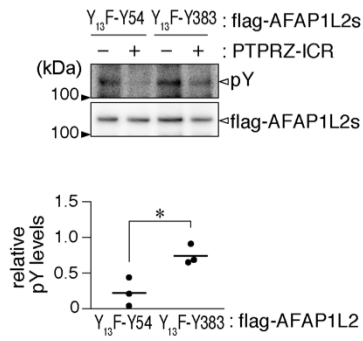


**Figure II-5 *In vitro* dephosphorylation of AFAP1L2 by PTPRZ.** FLAG-tagged AFAP1L2 F<sub>13</sub>-Y54 and -Y383 proteins purified by immunoprecipitation with anti-FLAG beads were incubated with human PTPRZ-ICR proteins, and tyrosine phosphorylation levels were examined, as shown in Figure II-2c. The scatter plot shows the signal intensity of PY20 staining relative to the non-treated control, in which each circle corresponds to an independent assay ( $n = 3$ ). \*,  $p < 0.05$ ; \*\*,  $p < 0.01$ , significant difference between the two groups by Welch's  $t$ -test.

## **Chapter III**

**AFAP1L2 is the key substrate molecule  
coupling PTN-PTPRZ signal to the PI3K-  
AKT pathway and involved in  
oligodendrocyte differentiation**

### **III .1 Introduction**

In the previous chapter, AFAP1L2 was identified as a substrate for PTPRZ. AFAP1L2 reportedly plays important roles in tumor progression by promoting cell proliferation, survival, motility and invasion in various cancer cells (Lodyga et al., 2010; Shiozaki et al., 2011). The PI3K-AKT-mTOR pathway is known to be involved in OPC differentiation and myelin formation (Cui et al., 2005; Kramer-Albers and White, 2011; Tyler et al., 2009; Yu et al., 2011). PTN-treated oligodendrocyte-lineage cells increased the phosphorylation of the substrate molecules of PTPRZ, such as p190 RhoGAP by the inhibition of PTPRZ, and significantly enhanced TH-induced differentiation to oligodendrocytes (Kuboyama et al., 2015). In order to investigate cellular functions of AFAP1L2 in OPC differentiation, I performed knockdown experiments with AFAP1L2 siRNA and investigate the role of AFAP1L2 in cell proliferation, survival, and differentiation under TH-induced differentiation conditions with or without PTN.

## **III. 2 Materials and methods**

### **Primary antibodies**

The commercially available antibodies used in the present study were as follows: anti-pS473 of AKT (Cell Signaling Technology, Danvers, MA, Cat# 4060), anti-AKT (Cell Signaling Technology, Cat# 9272), anti-pT202/pY204 of ERK1/2 (Cell Signaling Technology, Cat# 4370), anti-ERK (Cell Signaling Technology, Cat# 4695), anti-MBP (Santa Cruz Biotechnology, Cat# sc-13914), anti-NG2 proteoglycan (Millipore, Cat# AB5320), anti-pS2448 of mTOR (Cell Signaling Technology, Cat# 5536), and anti-mTOR (Cell Signaling Technology, Cat# 2983).

### **OL1 cell culture and siRNA transfection**

OL1 cells ( $2.0 \times 10^4$  cells) were cultured on a poly-*L*-ornithine-coated 3.5-cm plastic dish with “differentiation medium” containing knockout DMEM/F12 (cat #12660, Life Technologies), supplemented with 1× GlutaMAX (cat #35050, Life Technologies), 1× StemPro Neural Supplement (cat #A1050801, Life Technologies), 10 µg/ml of platelet-derived growth factor (PDGF-AA; cat #163–19731, Wako Pure Chemical), and 30 ng/ml thyronine and thyroxine (cat #T2752 and T2376, Sigma-Aldrich), or “basal medium”, and 10 µg/ml of PDGF-AA under a humidified chamber at 37°C with 5% CO<sub>2</sub>. Recombinant human PTN produced in yeast (Fukada et al., 2006) and LY294002 (cat #9901, Cell Signaling Technology) were used in the assay. In gene silencing experiments,  $5 \times 10^4$  cells cultured on a 3.5-cm dish for 5 days were transfected with 100 pmol of siRNA in 700 µl of

Opti-MEM using 3  $\mu$ l of HiPerFect Transfection Reagent (cat #301704, QIAGEN) according to the manufacturer's instructions. After 6 hrs, medium was changed to differentiation (or basal) medium for experiments. siRNAs were ordered and purchased from Nippongene, Tokyo, Japan. The AFAP1L2 sequences of siRNAs used were as follows: sense, 5'-UCACCAUGGUUAAGCUACA(dTdT)-3'; antisense, 5'-UGUAGCUUAACCAUGGUGA(dTdT). Universal Negative Control siRNA (Nippongene) was used as a negative control.

### **Rhotekin pull-down assays**

Active GTP-bound RhoA was precipitated from cell extracts using Rhotekin-RBD beads in a RhoA Pull-down Activation Assay Biochem Kit (cat #BK036, Cytoskeleton).

### **Immunocytofluorescence cell staining**

Cells were fixed with 4% paraformaldehyde in PBS (4.3 mM Na<sub>2</sub>HPO<sub>4</sub>, 1.4 mM KH<sub>2</sub>PO<sub>4</sub>, 137 mM NaCl, and 2.7 mM KCl at pH 7.4) for 30 min. Fixed cells were permeabilized and blocked with 4% non-fat dry milk and 0.1% Triton X-100 in TBS, and then incubated with the respective primary antibodies at 4°C overnight. Bound primary antibodies were visualized with Alexa Fluor-conjugated secondary antibodies (Life Technologies) by the standard procedure. Digital photomicrographs were taken with an LSM 700 confocal microscope (Zeiss).

### **Terminal deoxyribonucleotidyl transferase (TDT)-mediated dUTP-digoxigenin nick end labeling (TUNEL) assay**

In apoptosis assays, siRNAs were co-transfected with an mCherry expression plasmid (Fujikawa et al., 2015) to identify transfected cells. Apoptotic cells were identified using a TUNEL in situ apoptosis detection kit (Takara Bio) according to the manufacturer's instructions. Fluorescein (FITC)-labeled dUTP and mCherry signals were observed and photographed under a fluorescence microscope (Biozero BZ-8000, Keyence).

### **Cell Proliferation Assay**

The proliferation of OL1 cells was assessed by quantifying the incorporation of 5'-bromo-2-deoxyuridine (BrdU) using the cell proliferation ELISA BrdU kit (Roche) according to the manufacturer's instructions. BrdU incorporation was evaluated using a HRP-conjugated anti-BrdU antibody with tetramethylbenzidine (TMB) substrate. The absorbance of oxidized TMB was measured at 450 nm using a spectrofluorometer (FI-4500, Hitachi).

### III.3 Results

PTN reportedly stimulates the proliferation of several types of cancer cells through other receptors, including ALK (Papadimitriou et al., 2016). I examined the effects of suppressing AFAP1L2 expression in OL1 cells by siRNA knockdown (Figure III-1a). PTN significantly increased the incorporation of BrdU in OL1 cells; however, this was not affected by the knockdown of AFAP1L2 (Figure III-1b). I cannot exclude the possibility that the increased incorporation of BrdU is attributable to a *p53* deficiency in OL1 cells, which were established from *p53* knockout mice (Kuboyama et al., 2015). PI3K/AKT signaling plays a pivotal role in the suppression of apoptosis in multiple cell types (Hanahan and Weinberg, 2000). Consistently, the knockdown of AFAP1L2 significantly increased apoptosis in OL1 cells under differentiation conditions irrespective of the presence or absence of PTN (Figure III-1c). On the other hand, PTN induced AKT phosphorylation in OL1 cells (Figure III-1d), as previously reported in U87MG glioblastoma cells (Powers et al., 2002). However, the knockdown of AFAP1L2 prevented the PTN-induced phosphorylation of AKT (Figure III-1d) and mTOR (Figure III-1e), a downstream molecule of AKT, which correlated with the suppression of PTN-induced OL1 differentiation (Figure III-1f). These results suggest that AFAP1L2 couples the PTN signal to the activation of AKT and mTOR, thereby activating OL1 differentiation.

The PI3K inhibitor, LY294002 suppressed PTN-induced AKT phosphorylation in OL1 cells in a concentration-dependent manner (Figure III-2a): AKT phosphorylation returned to its baseline

level at 1.0  $\mu$ M. LY294002 at 1  $\mu$ M canceled both the enhancement in PTN-enhanced OL1 differentiation (Figure III-3a) and PTN-induced AKT phosphorylation (Figure III-3b). PTN also induced ERK1/2 phosphorylation and RhoA activation in OL1 cells, whereas LY294002 did not affect these responses (Figure III-2b), excluding the possibility of the non-specific actions of this reagent. These results suggested that AFAP1L2-dependent PI3K-AKT-mTOR activation is one of the key downstream reactions of PTN-PTPRZ signaling during OPC differentiation.

### **III. 4 Discussion**

In OL1 cells, the knockdown of AFAP1L2 increased apoptosis in OL1 cells, whereas PTN did not significantly affect apoptosis. And the knockdown of AFAP1L2 impaired PTN-induced AKT and mTOR phosphorylations and PTN-induced OPC differentiation. The inactivation of PI3K with wortmannin or LY294002 consistently impaired OPC differentiation to mature oligodendrocytes in primary cultures (Cui et al., 2005; Kramer-Albers and White, 2011), and the exogenous expression of constitutively active AKT in oligodendrocytes resulted in enhanced myelination in the CNS (Cui et al., 2005; Yu et al., 2011). LY294002 exerted similar effects to OL1 cells. PTN-induced PTPRZ inactivation was connected to the activation of the PI3K-AKT-mTOR pathway via AFAP1L2. In oligodendrocyte-lineage cells, AFAP1L2-dependent PI3K-AKT activation may be positively regulated by the kinase activity of FYN and negatively by the phosphatase activity of PTPRZ.

### III. 5 Figures

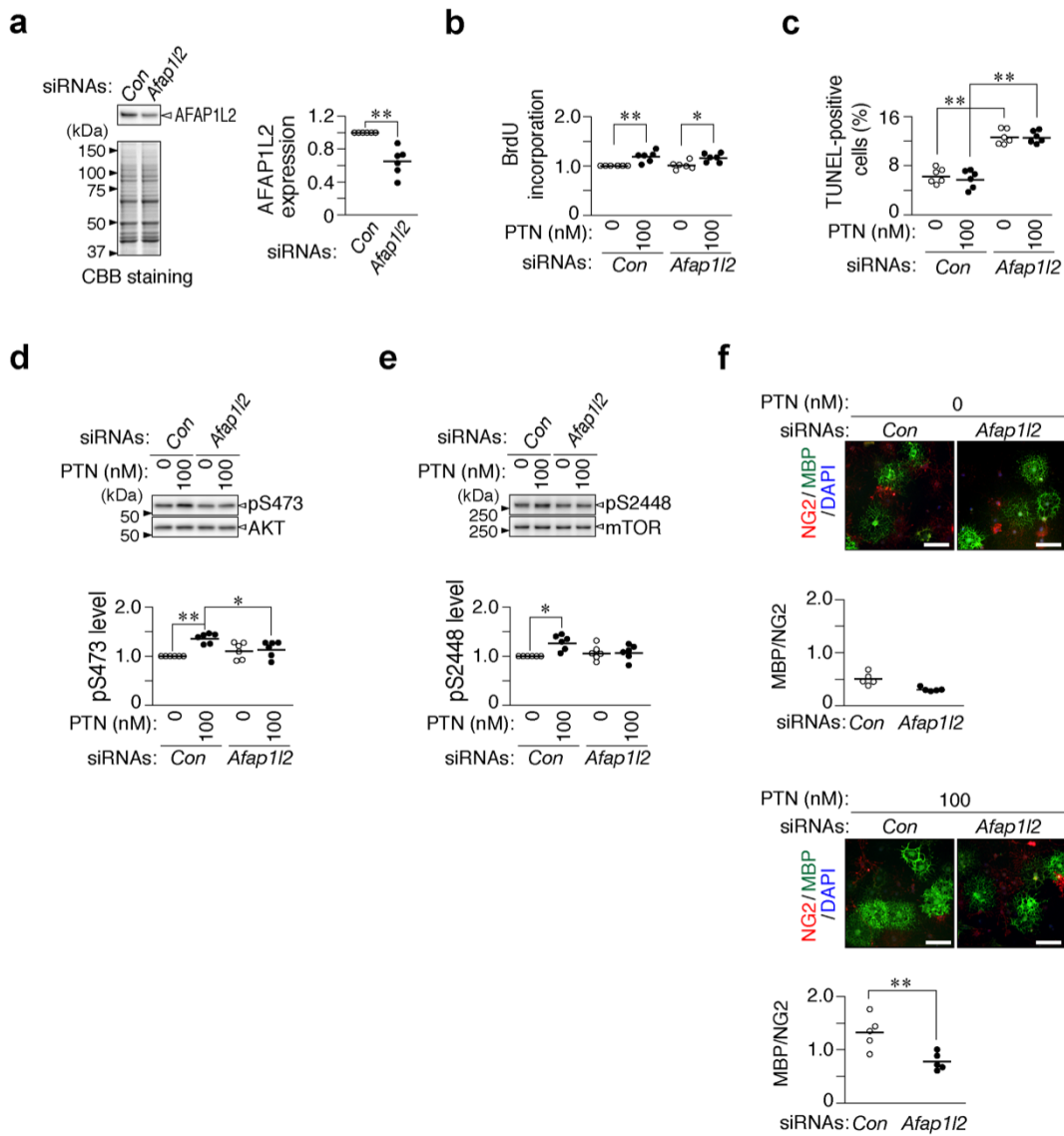


**Figure III-1 Effects of AFAP1L2 knockdown on OL1 cell properties.** (a) siRNA knockdown of AFAP1L2. siRNA targeted against AFAP1L2 (*Afap1/2*) or a control (*Con*) was transfected into OL1 cells. After 48 hrs of cultivation in basal medium, cell lysates were prepared. The *upper*

panel shows the amounts of AFAP1L2 proteins analyzed by Western blotting. The *lower* panel shows CBB staining of the proteins applied. The scatter plot shows the intensity of AFAP1L2 staining relative to the control cells from five independent experiments. \*\*,  $p < 0.01$ , significantly different from the control group by Welch's *t*-test. **(b,c)** Effects of AFAP1L2 knockdown on cell proliferation (*b*) and apoptosis (*c*). After 6 hrs of transfection, cells were cultured in differentiation medium with or without PTN for 2 days. Cell proliferation was evaluated by measuring the incorporation of BrdU for the last 12 hrs of the culture. Apoptotic cells were stained using the TUNEL method. Scatter plots show the relative levels of BrdU incorporation to the non-treated control group, and the percentage of FITC-labeled TUNEL-positive cells to siRNA-transfected, mCherry-positive cells, in which each circle corresponds to an independent experiment (BrdU incorporation,  $n = 3$  each; TUNEL staining,  $n = 6$  each). \*,  $p < 0.05$ ; \*\*,  $p < 0.01$ , significant difference between the indicated groups using a two-way ANOVA with Bonferroni's post hoc tests. **(d,e)** Effects of the AFAP1L2 knockdown on AKT and mTOR phosphorylation. After 48 hrs of transfection, cells were treated with or without PTN for 1 hr, and the phosphorylation levels of AKT at Ser-473 and amounts of AKT proteins, or the phosphorylation levels of mTOR at Ser-2448 and its protein amounts were analyzed using cell extracts. The scatter plot shows the intensity of pS473 (*d*) or pS2448 (*e*) staining relative to the control, in which each circle corresponds to an independent cell culture ( $n = 6$  each). \*,  $p < 0.05$ ; \*\*,  $p < 0.01$ , significant difference between the indicated groups using a two-way ANOVA with Bonferroni's post hoc tests. **(f)** Effects of AFAP1L2 knockdown on OL1 cell differentiation. After cell cultivation in differentiation medium with or without PTN for

10 days, cell differentiation was analyzed by staining with anti-NG2 proteoglycan (oligodendrocyte precursor cells, OPCs; *red*) and anti-MBP (oligodendrocyte; *green*) antibodies in conjunction with the DAPI labeling of nuclei (*blue*). *Scale bars*, 100  $\mu\text{m}$ . The scatter plot shows the ratio of MBP-positive cells to NG2-positive cells, with each circle corresponding to an independent cell culture ( $n = 5$  each). \*\*,  $p < 0.01$ , significant difference between the indicated groups using a two-way ANOVA with Bonferroni's post hoc tests.

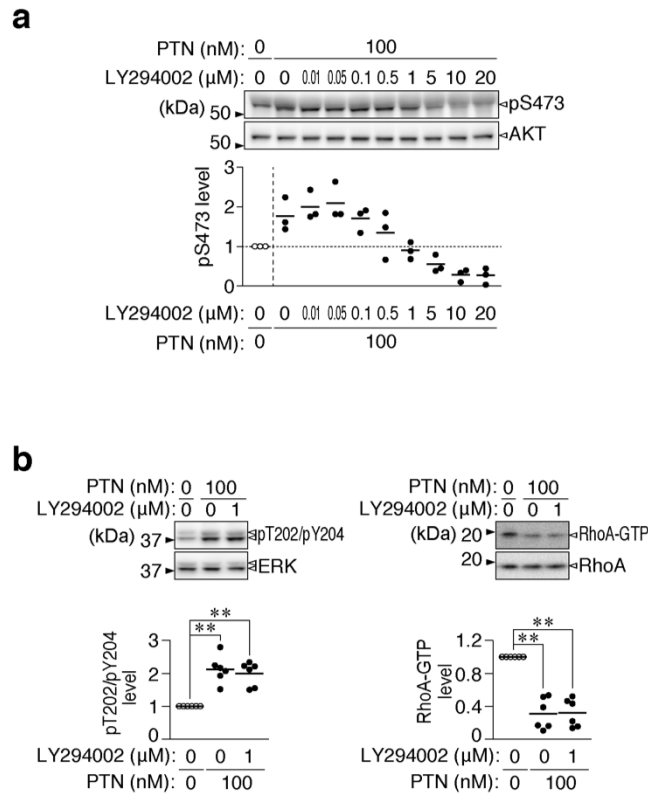


**Figure III-2 Effects of LY294002 on PTN-induced activation in AKT, ERK, or Rho in OL1 cells.**

**(a)** Effects of LY294002 on AKT phosphorylation. OL1 cells were treated with or without PTN for 1 hr, and the phosphorylation level of AKT at Ser-473 and amount of AKT proteins were analyzed using cell extracts. The scatter plot shows the intensity of pS473 staining relative to the control, in which each circle corresponds to an independent cell culture ( $n = 3$  each). **(b)**, Effects of LY294002 on ERK phosphorylation (*left*) and RhoA activation (*right*). OL1 cells were treated at the indicated combinations for 1 hr, and ERK phosphorylation in cell extracts was examined using a specific antibody against the phosphorylation site of ERK at Thr-202/Tyr-204 with an ERK antibody. The activation of RhoA was examined using the GST-Rhotekin pulldown assay. Scatter plots show the intensity of phospho-Thr-202/Tyr-204 or Rhotekin-bound RhoA (GTP-bound active form) bands

relative to the control, in which each circle corresponds to an independent cell culture ( $n = 6$  each).

\*\* $p < 0.01$  between the indicated groups using a one-way ANOVA with Bonferroni's post hoc tests.

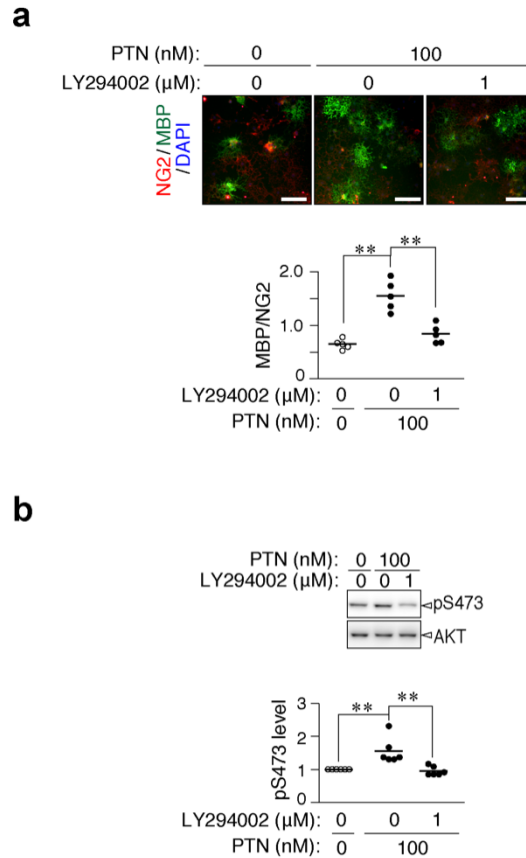


### Figure III-3 Involvement of the AKT-PI3K pathway in the PTN-induced differentiation of OL1

**cells.** (a) Effects of LY294002 on OL1 cell differentiation. OL1 cells were cultured in differentiation medium containing the indicated combinations of LY294002 (1  $\mu$ M) and PTN (100 nM) for 10 days, and their differentiation levels were analyzed by the staining of NG2 and MBP proteins, as in Figure III-1e. *Scale bars*, 100  $\mu$ m. The scatter plot shows the ratio of MBP-positive cells to NG2-positive cells, in which each circle corresponds to an independent cell culture ( $n = 5$  each). \*\*,  $p < 0.01$ , significant difference between the indicated groups using a two-way ANOVA with Bonferroni's post hoc tests. (b) Effects of LY294002 on AKT phosphorylation. OL1 cells were treated with the indicated combination for 1 hr, and AKT phosphorylation was analyzed, as shown in Figure III-1d. The scatter plot shows the intensity of pS473 staining relative to the control,

in which each circle corresponds to an independent cell culture ( $n = 6$  each). \*\*,  $p < 0.01$ , significant difference between the indicated groups using a two-way ANOVA with Bonferroni's post hoc tests.

## **Chapter IV**

# **Generation and phenotype analyses of mice carrying the inactive phosphatase knock-in mutation of PTPRZ**

## IV.1 Introduction

In developing mouse brains, the expression of the PTPRZ-A isoform peaks on approximately postnatal days 5 to 10 (P5 to P10), and the maximal expression of PTN occurs on P10, corresponding to the onset of myelination, whereas midkine and interleukin-34 are maintained at constant levels from the neonatal to adult stages (Kuboyama et al., 2016). *Ptprz*-deficient mice show the earlier onset of the expression of MBP, a major component of the myelin sheath, than wild-type mice (Kuboyama et al., 2012b); inversely, *Ptn*-deficient mice exhibit the later onset of MBP expression (Kuboyama et al., 2016). These findings indicate that the ligand-receptor pair of PTN-PTPRZ-A affects the timing of OPC differentiation in the developing brain (Kuboyama et al., 2016). The p190RhoGAP-Rho-ROCK pathway has been identified as a downstream of PTPRZ for OPC differentiation (Kuboyama et al., 2012b; Kuboyama et al., 2015; Kuboyama et al., 2016).

Previously, my laboratory reported the earlier onset of the expression of MBP, a major protein of the myelin sheath, as well as the earlier initiation of myelination in neonatal brains in *Ptprz*-deficient (null) mice than in wild-type mice (Kuboyama et al., 2012b). To assess the physiological significance of its PTPase activity, I newly generated a mouse line with a Cys-1930 to Ser (CS) point mutation in the *Ptprz* gene.

## **IV. 2 Materials and methods**

### **Primary antibodies.**

The commercially available antibodies used in the present study were as follows: anti-MYRF (Millipore Cat# ABN45), anti-OLIG2 (Millipore Cat# AB9610), and anti-RPTP $\beta$  (BD Biosciences Cat# 610180).

### **Ethics statement and experimental animals.**

All experimental animal protocols used in the present study were approved by the Institutional Animal Care and Use Committee of the National Institutes of Natural Sciences (approval numbers: 15A096, 16A145, and 16A148) and RIKEN Kobe Branch (approval number: A2001-03-72), Japan. *Ptprz*-deficient mice (Shintani et al., 1998) and *Ptprz*-CS mice (see below) were backcrossed with the inbred C57BL/6J strain (CLEA Japan) for more than ten generations. Mice were housed under specific pathogen-free (SPF) conditions at a constant room temperature (23°C) and 50–55% humidity with an 8:00 to 20:00 light cycle. Four to 5 weeks after birth, three to four sex-matched mice were housed in plastic cages (cage size: 12 × 21 × 12.5 cm) with paper-chip bedding, and food and water were provided ad libitum. Adult male mice (2 to 4 months old) and juvenile mice (< postnatal 30 days, gender unknown) were used in the present study. Mice were handled gently to minimize stress and were quickly decapitated without anesthesia to obtain tissue samples for biochemical analyses in this study. Paraformaldehyde fixation was performed under isoflurane anesthesia.

## Generation of the knock-in mouse

A *Ptprz* Cys1930 to Ser (CS) knock-in mouse (Accession No. CDB0971K: <http://www2.clst.riken.jp/arg/mutant%20mice%20list.html>) was generated as follows: Targeting gene sequences were isolated from a C57BL/6J BAC library (BACPAC) by a homologous recombination approach (Red/ET Recombineering, Gene Bridges), and inserted into a DT-A-pA/loxP/PGK-Neo-pA/loxP vector (LARGE, CDB, RIKEN <http://www2.clst.riken.jp/arg/cassette.html>). The mutation of Cys-1930 to Ser was performed using a commercial kit (KOD-Plus-Mutagenesis Kit, Toyobo): the positions of the amino acid residues were referred to that of the mouse PTPRZ-A isoform (Genbank; NM\_001081306).

Genotyping was performed on tail DNAs by PCR. The primers used were (for their positions, see Figure IV-1a); 5'-AGGTGAGTCTCAGAGCTGTTCTCCGA-3' (forward primer) and 5'-GTTTAAGAACAAAGCAGTGCTATGTCTGTC-3' (reverse primer). PCR products were 274 bp for the wild-type allele and 406 bp for the CS knock-in allele. PCR was performed with high yield Taq DNA polymerase (Jena Bioscience), 0.5  $\mu$ M primer pairs, and 100 ng tail DNAs in 15- $\mu$ l reactions. Cycling conditions were 94 °C for 180 s, 32 cycles of 94 °C for 15 s, 60 °C for 30 s, and 72 °C for 60 s, followed by a final extension step at 72°C for 420 s.

CS knock-in mice were backcrossed over ten generations with C57BL/6J mice. CS knock-in mice were fertile and viable and appeared indistinguishable from wild-type or *Ptprz*-deficient mice.

## **cDNA synthesis and quantitative real-time PCR**

Total RNA was isolated from brain tissues with TRIzol Reagent kit (Thermo Fisher Scientific). cDNAs were synthesized using the PrimeScript RT reagent Kit with gDNA Eraser (Takara Bio), and used as a template for real-time PCR using a commercial kit (TaKaRa One Step SYBR, Takara Bio) on a real-time PCR system (StepOnePlus Real-Time PCR System, RRID:SCR\_015805). The relative mRNA expression levels of the *Ptprz-A*, *-B*, and *-S* isoforms were calculated and normalized to that of glyceraldehyde-3-phosphate dehydrogenase (*Gapdh*). The PCR primers used and sizes of the amplified products were as follows: *Ptprz-A*; forward primer, 5'-CAGGAGTATCCAACAGTTCAGAG-3' and reverse primer, 5'-CTTCTCAGACTC CAACCCCTC-3' (89 bp). *Ptprz-B*; forward primer, 5'-CCTCCAGACCACTTGATTTG-3' and reverse primer for *Ptprz-A* (134 bp). *Ptprz-S*; forward primer, 5'-AACCAGAAC GTTCAACCATTTG-3' and reverse primer, 5'-GAATAGGAATTAGTAACAAC-3' (138 bp). *Gapdh*; forward primer, 5'-ATGGTGAAGGTCGGTGTG-3' and reverse primer, 5'-GTC GTT GATGGCAACAATC-3' (99 bp).

## **Immunohistochemistry staining**

Perfusion fixation was performed under isoflurane anesthesia, and removed brains were immediately immersed in 4% paraformaldehyde in PBS at 4°C overnight, followed by paraffin embedding. Four micrometer-thick deparaffinized sections were permeabilized and blocked with 4% non-fat dry milk and 0.1% Triton X-100 in TBS for 30 min, and then incubated with the respective primary antibodies

at 4°C overnight. Bound primary antibodies on tissue sections were visualized with HRP-conjugated secondary antibodies along with the Dako liquid diaminobenzidine (DAB) chromogen system (DAKO). Digital photomicrographs of individual specimens were taken with the Eclipse microscope Ci-L with DS-Fi2 CCD (Nikon).

### **Cuprizone-induced demyelination and micro-computed tomography**

Demyelination was induced in 2-month-old male mice by feeding powdered mouse chow containing 0.2% cuprizone (cat #. C9012, Sigma-Aldrich) for 6 weeks, and the normal pellet diet was then re-initiated for the induction of remyelination as described previously (Kuboyama et al., 2015; Kuboyama et al., 2017). Regarding micro-CT imaging, mouse brains were fixed with 4% paraformaldehyde and immersed in a graded series of Histodenz (cat #. D2158, Sigma-Aldrich) solutions. Specimens were scanned on the micro-CT system R\_mCT2 (Rigaku) at 90 kV (160  $\mu$ A) with a 20-mm field of view, and data were reconstructed using OsiriX software (OsiriX Medical Imaging Software). CT numbers were recorded from two regions of interest (four adjacent pixels each) in the dorsal corpus callosum and cerebral cortex for each image.

### IV.3 Results

Quantitative reverse transcription (RT)-PCR analyses revealed that the mRNA expression levels of the three splicing isoforms (*Ptprz-A*, *Ptprz-B*, and *Ptprz-S*) were similar in the brains of wild-type, heterozygous, and homozygous CS mutant mice (Figure IV-1b). Consistent with mRNA expression, no significant differences were observed in the Western blot patterns of brain extracts with specific antibodies against PTPRZ (Figure IV-1c to e). Thus, the CS mutation did not affect the expression profiles of PTPRZ isoforms. The full-length core protein (380 kDa) of PTPRZ-A was hardly detected, as already described (Chow et al., 2008b), despite significant expression at the mRNA level (see Figure IV-1b) (Chow et al., 2008b): PTPRZ proteins are targets for metalloproteinases (Chow et al., 2008b) and plasmin (Chow et al., 2008a) under physiological conditions, and are proteolytically cleaved into fragments, such as  $Z_A$ -ECF,  $Z_B$ -ECF, Z-ECF-100, -90, and -70, in the brain (Chow et al., 2008a; Chow et al., 2008b).

Immunohistochemical staining and Western blotting analyses revealed that CS knock-in mice as well as *Ptprz*-deficient mice showed stronger MBP expression in the corpus callosum on P10 than wild-type mice (Figure IV-2a,c); however, similar levels were reached by P90 (Figure IV-2b,d). Similar alterations were found in the protein expression level of the myelin regulatory factor MYRF (also known as MRF or Gm98), a critical transcriptional regulator that is essential for oligodendrocyte maturation and CNS myelination (Bujalka et al., 2013; Emery et al., 2009) (Figure IV-2e), while there were no genotypic differences in the expression of OLIG2, a pan-oligodendrocyte lineage marker

(Figure IV-2f). These results indicated that the regulation of OPC differentiation and myelination by PTPRZ is entirely dependent on its PTPase activity.

I then compared the phosphorylation levels of AFAP1L2, AKT, and mTOR among the three mouse groups. Consistent with MBP expression levels, the phosphorylation levels of AFAP1L2, AKT, and mTOR were significantly higher in CS knock-in mice and *Ptprz*-deficient mice than in wild-type mice on P10 (Figure IV-3a), while these genotypic differences disappeared at the adult stage (Figure IV-3b). Similar tyrosine phosphorylation patterns were observed in p190RhoGAP (Figure IV-3a,b), which is tyrosine phosphorylated by FYN for oligodendrocyte differentiation and myelination (Wolf et al., 2001), and is dephosphorylated by PTPRZ (Kuboyama et al., 2012b; Kuboyama et al., 2015; Kuboyama et al., 2016).

I further examined whether the PTPase of PTPRZ is also crucial for recovery from the cuprizone (a copper chelator) model of demyelination, which is induced by cuprizone feeding, because *Ptprz*-deficient mice show accelerated remyelination after the removal of cuprizone (Kuboyama et al., 2015). I performed the same experiments and found that CS knock-in mice showed similar levels of the acceleration of remyelination to those of *Ptprz*-deficient mice (Figure IV-4).

#### IV. 4 Discussion

My laboratory previously reported that *Ptprz*-deficient mice, which lack all three isoforms, exhibited the early onset of myelination in the developing brain and accelerated remyelination after demyelinating lesions (Kuboyama et al., 2012b; Kuboyama et al., 2015). OPC differentiation was shown to be inhibited on CSPG-coated culture dishes (Keough et al., 2016; Kuboyama et al., 2017). CSPGs, including aggrecan, versican, and neurocan, are enriched in demyelinating plaques in neurodegenerative diseases, such as multiple sclerosis (MS), and impair remyelination (Lau et al., 2012). It is important to note that the three PTPRZ isoforms are all CSPGs (Chow et al., 2008a; Chow et al., 2008b; Nishiwaki et al., 1998). Thus, the inhibitory activity of PTPRZ on OPC differentiation may partly be due to the function of chondroitin sulfate chains attached to the core protein of PTPRZ. However, the phenotypes of MBP expression and remyelination observed in phosphatase-inactive CS knock-in mice were similar to those in *Ptprz*-deficient mice (Figure IV-2 to 4).

Furthermore, the tyrosine phosphorylation levels of AFAP1L2 and p190RhoGAP were higher in CS knock-in mice, as well as in *Ptprz*-deficient mice, than in wild-type mice on P10 (Figure IV-3). These results indicate that the PTPase activity is predominantly involved in the PTN-PTPRZ-mediated regulatory mechanisms for OPC differentiation. On the other hand, Huang JK et al. reported accelerated axonal loss in another *Ptprz* knockout mouse line following lysolecithin-induced acute demyelination in the spinal cord (Huang et al., 2012). Since PTPRZ proteins are also

expressed in astrocytes and neurons (Shintani et al., 1998), I cannot exclude the possible effects of these cells on oligodendrocyte-lineage cells in knockout or CS knock-in *Ptprz* mutant mice.

Moreover, I demonstrated that CS knock-in mice and *Ptprz*-deficient mice exhibited similar phenotypes; the enhanced tyrosine phosphorylation of AFAP1L2 and p190RhoGAP along with the accelerated expression of MYRF and MBP in the developing brain, and accelerated remyelination in the adult brain in the cuprizone model. AFAP1L2 and p190RhoGAP (as well as ERBB4) exhibited expression peaks between P5 and P10 around the onset of myelination in mouse brains (Figure IV-5). PTPRZ-A, FYN, and PTN also reached their expression peaks on P5-10, P10, and P10, respectively (Kramer et al., 1999; Kuboyama et al., 2016). The expression of PTPRZ-A may prevents OPC differentiation by FYN until ~P10, and the blockage of PTPRZ is released by the expression of PTN. Thus, both AFAP1L2 and p190RhoGAP may be key downstream molecules of FYN and PTPRZ that regulate myelination during development.

## IV.5 Figures

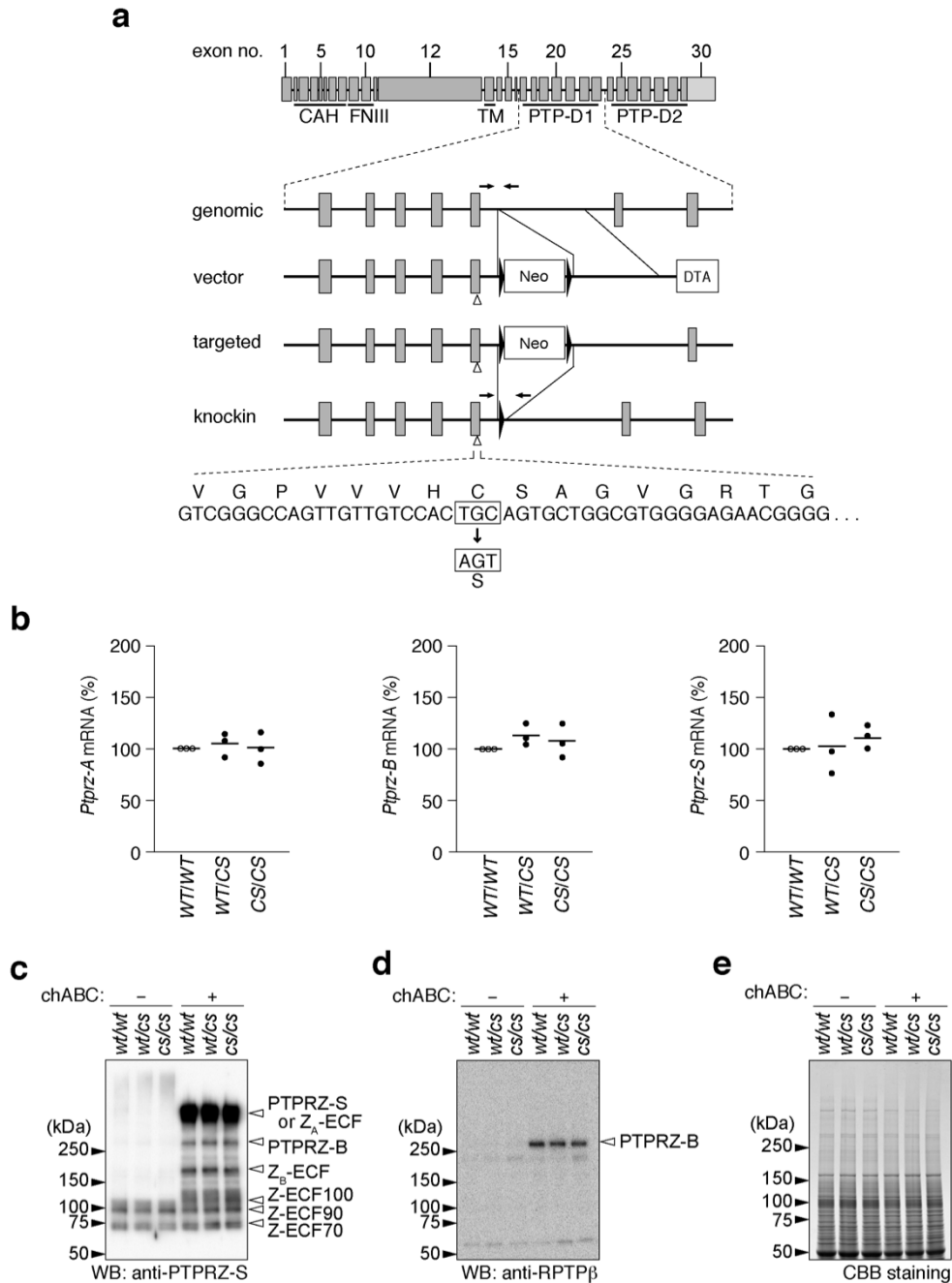


**Figure IV-1 *Ptprz* Cys1930 to Ser (CS) knock-in mouse.** (a) Strategy to generate a Cys1930 to Ser knock-in in the *Ptprz* gene. Schematic representation of the exon structure coding for the *Ptprz-A* isoform. Each box indicates an exon with the exon number, and the final exon 30 containing the 3'-non-coding sequence is shown in light gray. Horizontal arrows indicate primer sites for PCR genotyping. CAH, carbonic anhydrase-like domain; FNIII, fibronectin type III domain; TM, transmembrane region; PTP-D1 and -D2, tyrosine phosphatase domain 1 and 2. Neo, neomycin-resistance gene cassette; DTA, diphtheria toxin A gene cassette. (b) mRNA expression of *Ptprz* isoforms. *Ptprz-A*, *Ptprz-B*, and *Ptprz-S* mRNA levels in mouse brains (*wt/wt*, homozygous for the wild-type allele; *wt/cs*, heterozygous; and *cs/cs*, homozygous for the CS mutant allele) were measured by quantitative RT-PCR. They were normalized to *Gapdh* expression, and plotted as relative values to *wt/wt* mice ( $n = 3$  animals per group). (c-e) Protein expression of PTPRZ isoforms. In the brain, the three PTPRZ isoforms (PTPRZ-A, -B, and -S) and their processed derivatives ( $Z_A$ -ECF and  $Z_B$ -ECF) are expressed as CSPGs, and the removal of the chondroitin sulfate chains by the chABC treatment beforehand is necessary for resolving their core proteins by SDS-PAGE (Chow et al., 2008a; Chow et al., 2008b). Western blot analyses of brain extracts treated with (+) or without (-) chABC were performed using anti-PTPRZ-S (c), which recognizes the extracellular region of all three isoforms, and anti-RPTP $\beta$  (d), which recognizes the PTP-D2 region. The protein amounts applied were verified by CBB staining (e).

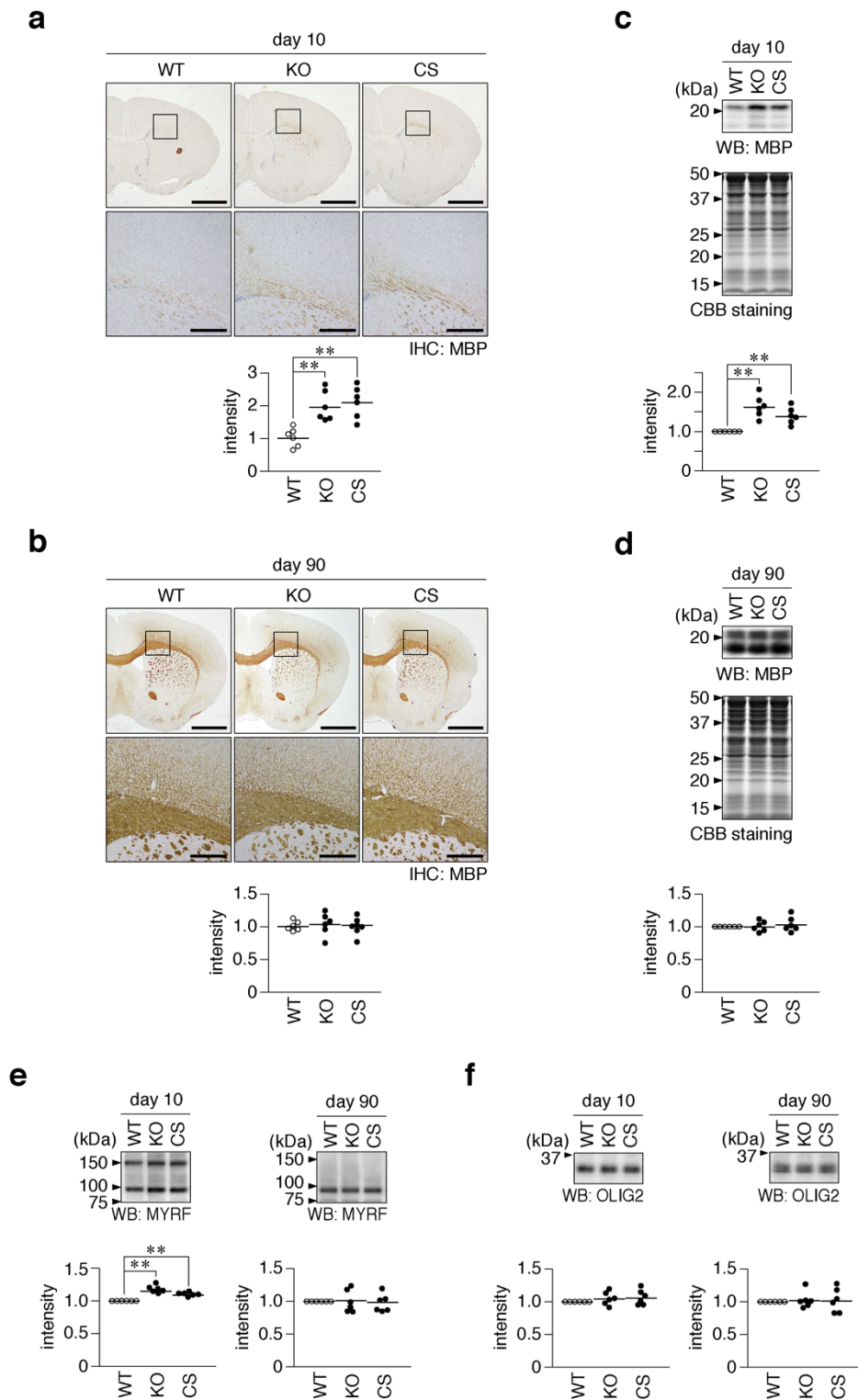


**Figure IV-2 Expression of oligodendrocyte markers in *Ptpz* mutant mouse brains.** (a,b) Anti-MBP staining of mouse brain tissue sections on postnatal days 10 (a) and 90 (b). Images show the immunohistochemical (IHC) staining of wild-type (WT), *Ptpz*-deficient (KO), *Ptpz* Cys-1930 to

Ser mutant knock-in (CS) mouse brains. The *bottom* images are enlarged views of the rectangular regions in the *top* panels. *Scale bars*, 1 mm (*top pictures*) and 200  $\mu\text{m}$  (*bottom pictures*), respectively. The scatter plot shows the arbitrary densitometric units of the intensity of MBP staining in the corpus callosum in each animal normalized to the average of the WT group ( $n = 6$  animals per group). \*\*,  $p < 0.01$ , significantly different from the WT mouse using a one-way ANOVA with Dunnett's post hoc test. **(c,d)** Amounts of MBP proteins on postnatal days 10 (c) and 90 (d). The panels show the Western blotting of the cerebral cortices of WT, KO, and CS mouse brains with the CBB staining of applied proteins. Murine MBP has four isoforms (21.5 to 14 kDa), the expression patterns of which change during development (Boggs, 2006). All MBP bands detected were quantified in total relative to the WT in each experiment ( $n = 6$  animals per group). \*\*,  $p < 0.01$ , significantly different from the WT group using a one-way ANOVA with Dunnett's post hoc test. **(e,f)** Western blotting of MYRF proteins (e) and OLIG2 (f) in WT, KO, and CS mouse brains on postnatal days 10 and 90. MYRF proteins exist as the full-length ( $\sim 150$  kDa) and a truncated cleavage product ( $\sim 80$  kDa) (Bujalka et al., 2013), and, thus, all MYRF bands detected were quantified in total. The scatter plot shows signal intensities relative to the control, in which each circle represents a relative value to the WT in each experiment ( $n = 6$ ). \*\*,  $p < 0.01$ , significantly different from the WT group using a one-way ANOVA with Dunnett's post hoc test.

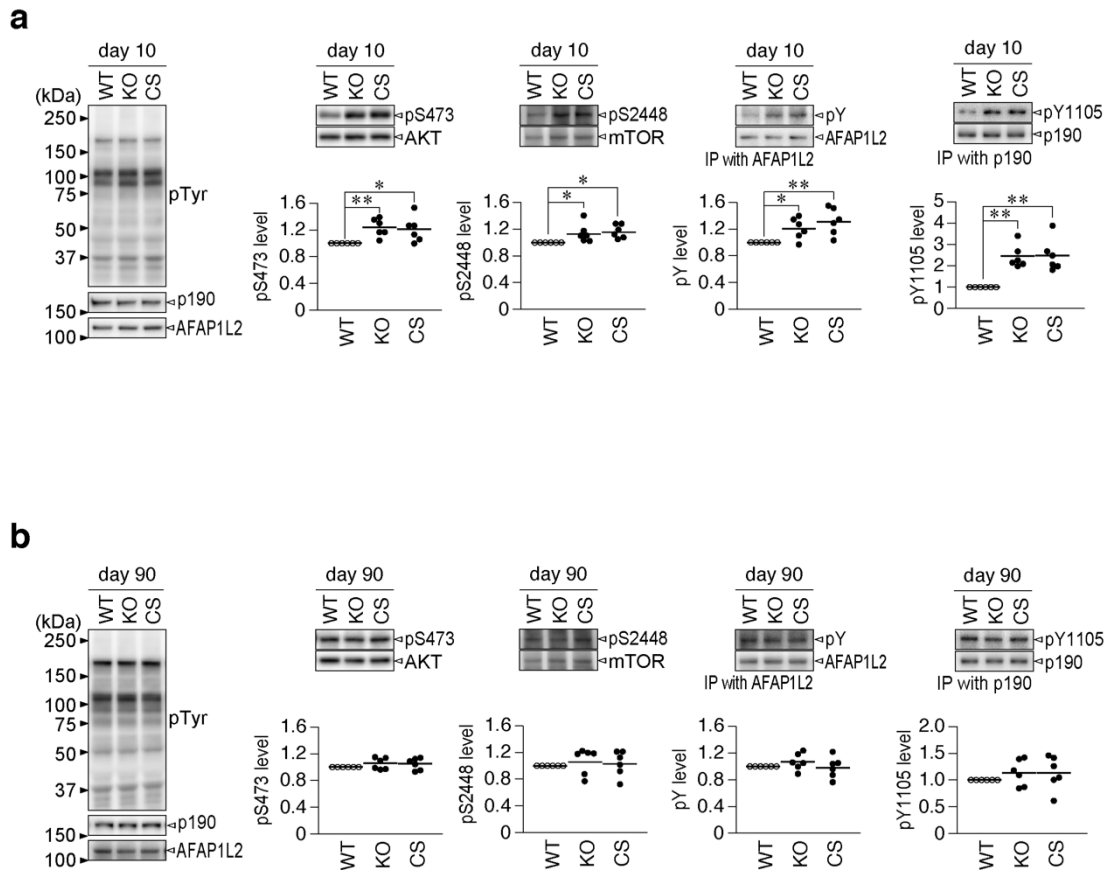


**Figure IV-3 AKT, AFAP1L2, and p190RhoGAP phosphorylation in mouse brains. (a,b)**

Phosphorylation levels of AKT, mTOR, AFAP1L2, and p190RhoGAP on postnatal days 10 (a) and 90 (b). Brain extracts prepared from WT, KO, and CS mice were subjected to analyses of overall tyrosine phosphorylation patterns, and the protein amounts of AFAP1L2 and p190RhoGAP (*the most-left panels*). Phosphorylation levels of AKT and mTOR (*the second and third panels from the left*) were examined using cell extracts, and the tyrosine phosphorylation levels of AFAP1L2 (*third panels from the left*) and p190RhoGAP (*the most-right panels*) were investigated in the immunoprecipitates of brain extracts. Scatter plots show signal intensities normalized to wild-type

controls ( $n = 6$  animals per group). \*,  $p < 0.05$ ; \*\*,  $p < 0.01$ , significantly different from the WT group using a one-way ANOVA with Dunnett's post hoc test.

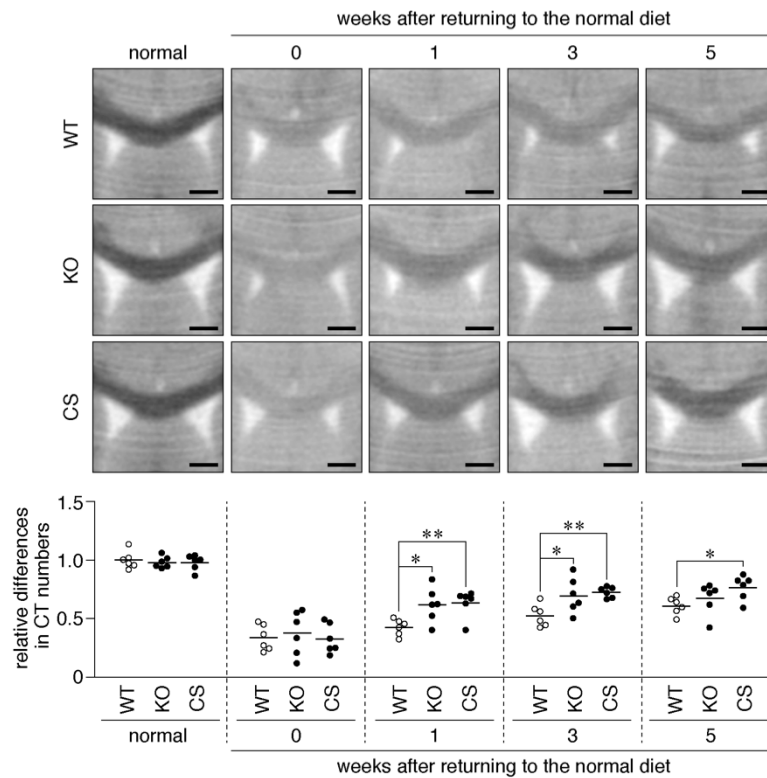


**Figure IV-4 Remyelination after cuprizone-induced demyelination.** Micro-computed tomography (micro-CT) images of cuprizone-treated mouse brains. Mice were fed a cuprizone-containing diet for 6 weeks (*0 weeks*) to induce demyelination, followed by spontaneous remyelination with the removal of cuprizone from the diet (*1, 3, and 5 weeks*). *Normal* mice were maintained on the regular diet. Images show the coronal plane reconstruction of micro-CT scans of the dorsal corpus callosum of Histodenz-immersed brains derived from WT, KO, and CS mice. *Scale bars*, 1 mm. After feeding the cuprizone-containing diet, differences between CT numbers in the dorsal corpus callosum and cerebral cortex decreased because demyelinated areas showed high penetration of the contrast reagent (compare “*normal*” vs “*0*”)(Kuboyama et al., 2015). Damage gradually recovered after a return to the normal diet (compare “*0*” vs “*1*”, “*3*”, and “*5*”). The *lower*

scatter plots show relative differences normalized to the averaged value of normal diet-fed wild-type mice ( $n = 6$  animals per group). Each circle corresponds to the average value of the two regions from an individual mouse. \*,  $p < 0.05$ ; \*\*,  $p < 0.01$ , significantly different from the WT group using a one-way ANOVA with Dunnett's post hoc test.

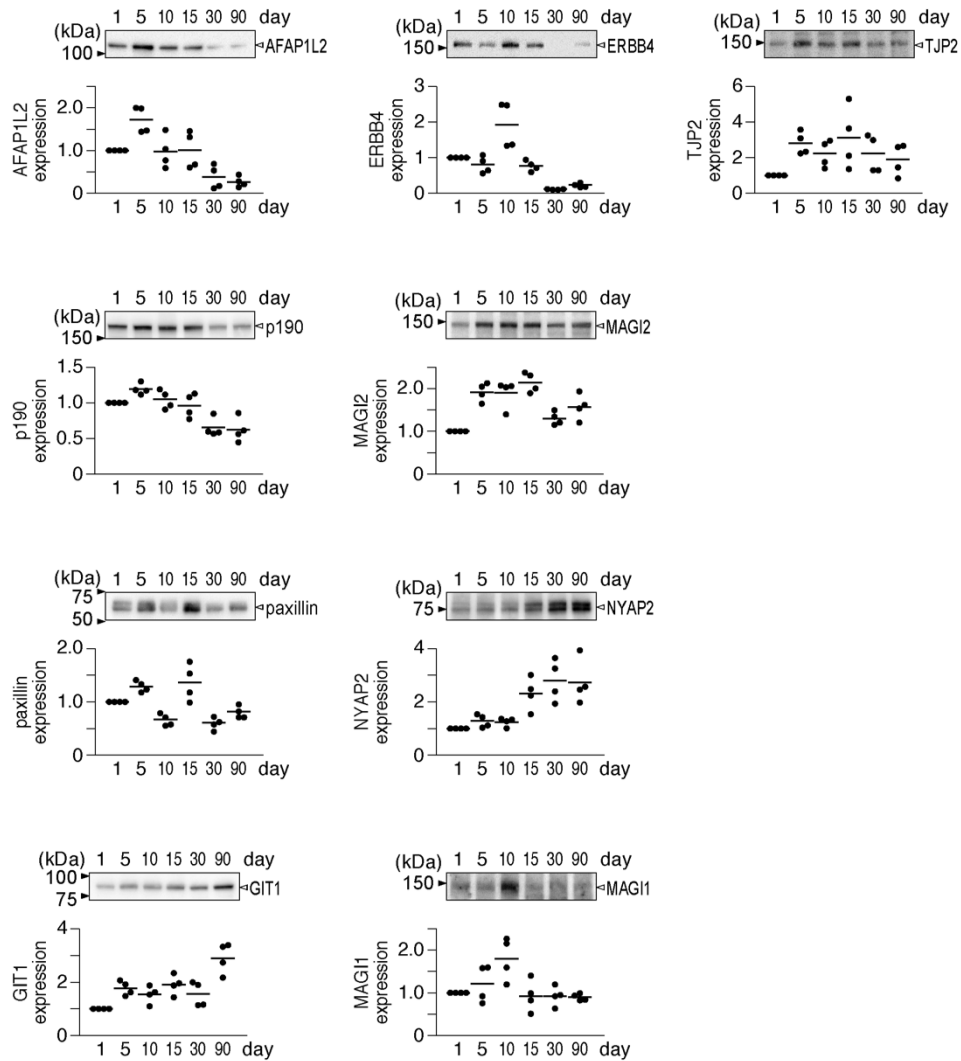


**Figure IV-5 Developmental expression profiles of target candidate molecules of PTN-PTPRZ**

**signaling in the mouse brain.** Tissue extracts prepared from the brain tissues of C57BL/6J mice at the respective postnatal days were subjected to Western blotting analyses using specific antibodies against each indicated protein. The scatter plots below each blot show the arbitrary densitometric units of the signal intensity normalized to the value on postnatal day 1 ( $n = 4$  per each age).

# **Chapter V**

## **Summary and conclusion**

## V. 1 Discussion

In this study, I revealed that AFAP1L2 was a major PTPRZ substrate, and PTPRZ efficiently dephosphorylated at Tyr-54 as the primary site involved in the binding of p85 $\alpha$  to AFAP1L2. PTN-PTPRZ signal increased the Tyr-phosphorylation level in AFAP1L2 and thereby activated the PI3K-AKT-mTOR pathway for oligodendrocyte differentiation. I here summarize other tyrosine phosphorylation-enhanced molecules by the PTN stimulation than AFAP1L2 and discuss about their conceivable roles in oligodendrocyte differentiation (Figure V-1). Among the substrate molecules for PTPRZ previously identified, PTN-induced tyrosine phosphorylation was detected in GIT1, paxillin, and ERBB4 in OL1 cells (see Figure II-1).

GIT1 functions as a scaffold for MEK1 to activate ERK1/2 in focal adhesions, which regulates cell migration (Yin et al., 2004; Yin et al., 2005). Src activates GIT1 and stimulates its association with ERK in focal adhesions. In A7r5 smooth muscle cells, cyclic phosphorylation/dephosphorylation at Tyr-554 in GIT1 (by Src and PTPRZ) is crucial for coordinated cell motility, which is regulated through dynamic interactions between GIT1 and paxillin/Hic-5 (Fujikawa et al., 2015).

Paxillin associates with ERK through the Src-mediated phosphorylation of Tyr-118 in paxillin (Ishibe et al., 2003), which is the dephosphorylation site by PTPRZ (Fujikawa et al., 2011). Tyr-118 phosphorylation by Src regulates the hepatocyte growth factor (HGF)-stimulated ERK association, which is critical for HGF-stimulated epithelial morphogenesis, including cell spreading

and process branching (Ishibe et al., 2003). Thus, GIT1 and paxillin may function as scaffold proteins to enhance the MEK-ERK pathway in oligodendrocyte differentiation.

Previous studies suggested that the neureglin1 (NRG1)–ERBB4 signal prevents apoptosis and enhances the survival of OPCs during differentiation (Colognato et al., 2004; Nave and Salzer, 2006). Axonally-bound or secreted NRG1 binds to ERBB, and promotes OPC survival by activating the PI3K-AKT pathway (Mitew et al., 2014). However, in the presence of laminins on myelinating axon tracts, ERBB receptors associate with  $\alpha6\beta1$  integrins in the plasma membrane of OPCs and stimulate MAPK-driven differentiation signals (Colognato et al., 2004). Fyn-depleted oligodendrocytes do not show increases in survival in response to NRG1 (Colognato et al., 2004), indicating that the survival signal driven by laminin and NRG requires FYN. Previous studies reported that PTN and its family member, midkine, bound to integrins (Mikelis et al., 2009; Muramatsu et al., 2004), and midkine promoted the complex formation of PTPRZ with  $\alpha6\beta1$  or  $\alpha4\beta1$  integrins (Muramatsu et al., 2004). PTPRZ/Integrin/ERBB4 may form multiple receptor complexes during OPC differentiation.

Although there is currently no evidence to show the dephosphorylation of NYAP2 by PTPRZ, this may also be important. NYAP2 is a member of a Neuronal Tyrosine- phosphorylated Adaptor for the PI3K family (NYAP), which is predominantly expressed in neurons (Yokoyama et al., 2011); almost no expression was observed in rat CG4 oligodendrocyte cells, whereas NYAP2 was expressed in mouse oligodendrocyte-lineage OL1 cells. Of note, tyrosine phosphorylation was enhanced by PTN (Figure II-1), NYAPs are tyrosine-phosphorylated by FYN, phosphorylated NYAPs interact

with the p85 $\alpha$  subunit of PI3K and activate PI3K, and this links PI3K signaling to the WAVE1 complex (Yokoyama et al., 2011). Future studies are needed to establish whether NYAP2 has similar functions to AFAP1L2.

Previous studies reported that malignant gliomas strongly expressed PTPRZ (Muller et al., 2003; Ulbricht et al., 2003). As more clinically relevant findings, it was recently reported that transcripts encoding PTPRZ were highly expressed in individual cells by single-cell RNA sequencing of primary human glioblastomas, and analyses of intratumoral heterogeneity annotated PTPRZ as the major positive regulator of cancer stemness *in vivo* (Patel et al., 2014). PTPRZ has been shown to play roles in cell migration and adhesion in variegated cells including neuronal, glial, and gastric mucosal cells (Fujikawa et al., 2015; Fujikawa et al., 2003; Maeda and Noda, 1998). *Ptprz*-knockdown glioblastoma cells exhibited decreases in cell migration and proliferation *in vitro* and tumor size *in vivo* (Bourgonje et al., 2014; Foehr et al., 2006; Fujikawa et al., 2015; Fujikawa et al., 2003; Muller et al., 2003; Nishiwaki et al., 1998; Patel et al., 2014; Ulbricht et al., 2003; Ulbricht et al., 2006). On the other hand, pathway analysis showed that the top ranked disease related to AFAP1L2 is cancer, and the top molecular and cellular functions are cellular growth and proliferation, and cell cycle (Shiozaki et al., 2011). This time I identified AFAP1L2-mediated coupling of the PTN-PTPRZ signal to the PI3K-AKT pathway. This finding may provide new findings in cancer research as well.

In summary, I revealed that the PTN-PTPRZ signal stimulates OPC differentiation partly by enhancing the tyrosine phosphorylation of AFAP1L2 to activate the PI3K-AKT pathway. PTN-induced PTPRZ inactivation regulates multiple signaling pathways, in cooperation with FYN kinase, as a hub molecule that is essential for oligodendrocyte differentiation and myelination.

## V.2 Figure

*Pathways for OPC differentiation and myelination*

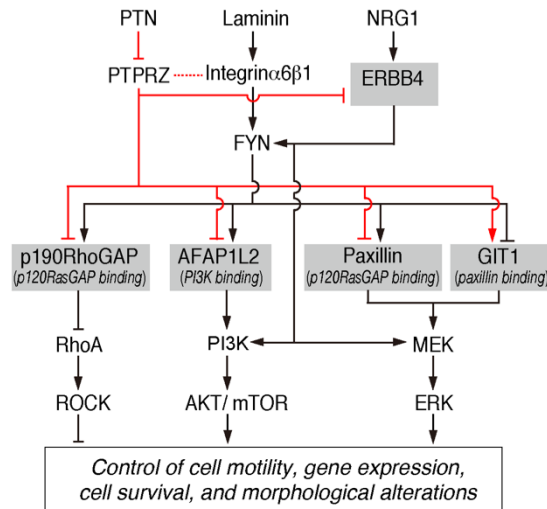


**Figure V-1 Proposed target molecules mediating the PTN-PTPRZ signal downstream.**

Detailed explanations and interpretations are provided in the Discussion section. Arrows indicate the activation and blunt arrows indicate the inhibition of target molecule function. PTPRZ substrate molecules are marked with gray boxes.

## References

- Andersen, J.N., O.H. Mortensen, G.H. Peters, P.G. Drake, L.F. Iversen, O.H. Olsen, P.G. Jansen, H.S. Andersen, N.K. Tonks, and N.P. Moller. 2001. Structural and evolutionary relationships among protein tyrosine phosphatase domains. *Mol Cell Biol.* 21:7117-7136.
- Barr, A.J., E. Ugochukwu, W.H. Lee, O.N. King, P. Filippakopoulos, I. Alfano, P. Savitsky, N.A. Burgess-Brown, S. Müller, and S. Knapp. 2009. Large-scale structural analysis of the classical human protein tyrosine phosphatome. *Cell.* 136:352-363.
- Boggs, J.M. 2006. Myelin basic protein: a multifunctional protein. *Cell Mol Life Sci.* 63:1945-1961.
- Bourgonje, A.M., A.C. Navis, J.T.G. Schepens, K. Verrijp, L. Hovestad, R. Hilhorst, S. Harroch, P. Wesseling, W.P.J. Leenders, and W.J.A.J. Hendriks. 2014. Intracellular and extracellular domains of protein tyrosine phosphatase PTPRZ-B differentially regulate glioma cell growth and motility. *Oncotarget.* 5:8690-8702.
- Buffo, A., and F. Rossi. 2013. Origin, lineage and function of cerebellar glia. *Prog Neurobiol.* 109:42-63.
- Bujalka, H., M. Koenning, S. Jackson, V.M. Perreau, B. Pope, C.M. Hay, S. Mitew, A.F. Hill, Q.R. Lu, M. Wegner, R. Srinivasan, J. Svaren, M. Willingham, B.A. Barres, and B. Emery. 2013. MYRF is a membrane-associated transcription factor that autoproteolytically cleaves to directly activate myelin genes. *PLoS Biol.* 11:e1001625.
- Canoll, P.D., S. Petanceska, J. Schlessinger, and J.M. Musacchio. 1996. Three forms of RPTP-beta are differentially expressed during gliogenesis in the developing rat brain and during glial cell differentiation in culture. *J Neurosci Res.* 44:199-215.
- Chow, J.P., A. Fujikawa, H. Shimizu, and M. Noda. 2008a. Plasmin-mediated processing of protein tyrosine phosphatase receptor type Z in the mouse brain. *Neurosci Lett.* 442:208-212.
- Chow, J.P., A. Fujikawa, H. Shimizu, R. Suzuki, and M. Noda. 2008b. Metalloproteinase- and gamma-secretase-mediated cleavage of protein-tyrosine phosphatase receptor type Z. *J Biol Chem.* 283:30879-30889.
- Chow, J.P.H., A. Fujikawa, H. Shimizu, R. Suzuki, and M. Noda. 2008c. Metalloproteinase- and gamma-Secretase-mediated Cleavage of Protein-tyrosine Phosphatase Receptor Type Z. *J Biol Chem.* 283:30879-30889.
- Colognato, H., S. Ramachandrapa, I.M. Olsen, and C. ffrench-Constant. 2004. Integrins direct Src family kinases to regulate distinct phases of oligodendrocyte development. *J Cell Biol.* 167:365-375.
- Cui, Q.L., W.H. Zheng, R. Quirion, and G. Almazan. 2005. Inhibition of Src-like kinases reveals Akt-dependent and -independent pathways in insulin-like growth factor I-mediated oligodendrocyte progenitor survival. *J Biol Chem.* 280:8918-8928.
- Emery, B., D. Agalliu, J.D. Cahoy, T.A. Watkins, J.C. Dugas, S.B. Mulinyawe, A. Ibrahim, K.L. Ligon, D.H. Rowitch, and B.A. Barres. 2009. Myelin gene regulatory factor is a critical transcriptional regulator required for CNS myelination. *Cell.* 138:172-185.

- Flores, A.I., S.P. Narayanan, E.N. Morse, H.E. Shick, X. Yin, G. Kidd, R.L. Avila, D.A. Kirschner, and W.B. Macklin. 2008. Constitutively active Akt induces enhanced myelination in the CNS. *J Neurosci.* 28:7174-7183.
- Foehr, E.D., G. Lorente, J. Kuo, R. Ram, K. Nikolich, and R. Urfer. 2006. Targeting of the receptor protein tyrosine phosphatase beta with a monoclonal antibody delays tumor growth in a glioblastoma model. *Cancer Res.* 66:2271-2278.
- Fujikawa, A., J.P. Chow, H. Shimizu, M. Fukada, R. Suzuki, and M. Noda. 2007a. Tyrosine phosphorylation of ErbB4 is enhanced by PSD95 and repressed by protein tyrosine phosphatase receptor type Z. *J Biochem.* 142:343-350.
- Fujikawa, A., J.P.H. Chow, M. Matsumoto, R. Suzuki, K. Kuboyama, N. Yamamoto, and M. Noda. 2017a. Identification of novel splicing variants of protein tyrosine phosphatase receptor type Z. *J Biochem.* 162:381-390.
- Fujikawa, A., J.P.H. Chow, H. Shimizu, M. Fukada, R. Suzuki, and M. Noda. 2007b. Tyrosine phosphorylation of ErbB4 is enhanced by PSD95 and repressed by protein tyrosine phosphatase receptor type Z. *J Biochem.* 142:343-350.
- Fujikawa, A., M. Fukada, Y. Makioka, R. Suzuki, J.P. Chow, M. Matsumoto, and M. Noda. 2011. Consensus substrate sequence for protein-tyrosine phosphatase receptor type Z. *J Biol Chem.* 286:37137-37146.
- Fujikawa, A., M. Matsumoto, K. Kuboyama, R. Suzuki, and M. Noda. 2015. Specific dephosphorylation at tyr-554 of git1 by ptpz promotes its association with paxillin and hic-5. *Plos One.* 10:e0119361.
- Fujikawa, A., A. Nagahira, H. Sugawara, K. Ishii, S. Imajo, M. Matsumoto, K. Kuboyama, R. Suzuki, N. Tanga, M. Noda, S. Uchiyama, T. Tomoo, A. Ogata, M. Masumura, and M. Noda. 2016. Small-molecule inhibition of PTPRZ reduces tumor growth in a rat model of glioblastoma. *Sci Rep.* 6:20473.
- Fujikawa, A., and M. Noda. 2016. Role of pleiotrophin-protein tyrosine phosphatase receptor type Z signaling in myelination. *Neural Regen Res.* 11:549-551.
- Fujikawa, A., D. Shirasaka, S. Yamamoto, H. Ota, K. Yahiro, M. Fukada, T. Shintani, A. Wada, N. Aoyama, T. Hirayama, H. Fukamachi, and M. Noda. 2003. Mice deficient in protein tyrosine phosphatase receptor type Z are resistant to gastric ulcer induction by VacA of *Helicobacter pylori*. *Nat Genet.* 33:375-381.
- Fujikawa, A., H. Sugawara, T. Tanaka, M. Matsumoto, K. Kuboyama, R. Suzuki, N. Tanga, A. Ogata, M. Masumura, and M. Noda. 2017b. Targeting PTPRZ inhibits stem cell-like properties and tumorigenicity in glioblastoma cells. *Sci Rep.* 7:5609.
- Fukada, M., A. Fujikawa, J.P. Chow, S. Ikematsu, S. Sakuma, and M. Noda. 2006. Protein tyrosine phosphatase receptor type Z is inactivated by ligand-induced oligomerization. *Febs Lett.* 580:4051-4056.
- Fukada, M., H. Kawachi, A. Fujikawa, and M. Noda. 2005. Yeast substrate-trapping system for isolating substrates of protein tyrosine phosphatases: Isolation of substrates for protein tyrosine phosphatase receptor type z. *Methods.* 35:54-63.

- Funfschilling, U., L.M. Supplie, D. Mahad, S. Boretius, A.S. Saab, J. Edgar, B.G. Brinkmann, C.M. Kassmann, I.D. Tzvetanova, W. Mobius, F. Diaz, D. Meijer, U. Suter, B. Hamprecht, M.W. Sereda, C.T. Moraes, J. Frahm, S. Goebbels, and K.A. Nave. 2012. Glycolytic oligodendrocytes maintain myelin and long-term axonal integrity. *Nature*. 485:517-521.
- Goebbels, S., J.H. Oltrogge, R. Kemper, I. Heilmann, I. Bormuth, S. Wolfer, S.P. Wichert, W. Mobius, X. Liu, C. Lappe-Siefke, M.J. Rossner, M. Groszer, U. Suter, J. Frahm, S. Boretius, and K.A. Nave. 2010. Elevated phosphatidylinositol 3,4,5-trisphosphate in glia triggers cell-autonomous membrane wrapping and myelination. *J Neurosci*. 30:8953-8964.
- Griffiths, I., M. Klugmann, T. Anderson, D. Yool, C. Thomson, M.H. Schwab, A. Schneider, F. Zimmermann, M. McCulloch, N. Nadon, and K.A. Nave. 1998. Axonal swellings and degeneration in mice lacking the major proteolipid of myelin. *Science*. 280:1610-1613.
- Hanahan, D., and R.A. Weinberg. 2000. The hallmarks of cancer. *Cell*. 100:57-70.
- Hornbeck, P.V., B. Zhang, B. Murray, J.M. Kornhauser, V. Latham, and E. Skrzypek. 2015. PhosphoSitePlus, 2014: mutations, PTMs and recalibrations. *Nucleic Acids Res*. 43:D512-520.
- Huang, J.K., C.C. Ferrari, G. Monteiro de Castro, D. Lafont, C. Zhao, P. Zaratini, S. Pouly, B. Greco, and R.J. Franklin. 2012. Accelerated axonal loss following acute CNS demyelination in mice lacking protein tyrosine phosphatase receptor type Z. *Am J Pathol*. 181:1518-1523.
- Ishibe, S., D. Joly, X. Zhu, and L.G. Cantley. 2003. Phosphorylation-dependent paxillin-ERK association mediates hepatocyte growth factor-stimulated epithelial morphogenesis. *Mol Cell*. 12:1275-1285.
- Kawachi, H., A. Fujikawa, N. Maeda, and M. Noda. 2001. Identification of GIT1/Cat-1 as a substrate molecule of protein tyrosine phosphatase zeta /beta by the yeast substrate-trapping system. *Proc Natl Acad Sci U S A*. 98:6593-6598.
- Kawachi, H., H. Tamura, I. Watakabe, T. Shintani, N. Maeda, and M. Noda. 1999. Protein tyrosine phosphatase zeta/RPTPbeta interacts with PSD-95/SAP90 family. *Brain Res Mol Brain Res*. 72:47-54.
- Keough, M.B., J.A. Rogers, P. Zhang, S.K. Jensen, E.L. Stephenson, T. Chen, M.G. Hurlbert, L.W. Lau, K.S. Rawji, J.R. Plemel, M. Koch, C.C. Ling, and V.W. Yong. 2016. An inhibitor of chondroitin sulfate proteoglycan synthesis promotes central nervous system remyelination. *Nature communications*. 7:11312.
- Kramer, E.M., C. Klein, T. Koch, M. Boytinck, and J. Trotter. 1999. Compartmentation of Fyn kinase with glycosylphosphatidylinositol-anchored molecules in oligodendrocytes facilitates kinase activation during myelination. *J Biol Chem*. 274:29042-29049.
- Kramer-Albers, E.M., and R. White. 2011. From axon-glia signalling to myelination: the integrating role of oligodendroglial Fyn kinase. *Cell Mol Life Sci*. 68:2003-2012.
- Kuboyama, K., A. Fujikawa, M. Masumura, R. Suzuki, M. Matsumoto, and M. Noda. 2012a. Protein Tyrosine Phosphatase Receptor Type Z Negatively Regulates Oligodendrocyte Differentiation and Myelination. *Plos One*. 7.

- Kuboyama, K., A. Fujikawa, M. Masumura, R. Suzuki, M. Matsumoto, and M. Noda. 2012b. Protein tyrosine phosphatase receptor type z negatively regulates oligodendrocyte differentiation and myelination. *Plos One*. 7:e48797.
- Kuboyama, K., A. Fujikawa, R. Suzuki, and M. Noda. 2015. Inactivation of Protein Tyrosine Phosphatase Receptor Type Z by Pleiotrophin Promotes Remyelination through Activation of Differentiation of Oligodendrocyte Precursor Cells. *J Neurosci*. 35:12162-12171.
- Kuboyama, K., A. Fujikawa, R. Suzuki, N. Tanga, and M. Noda. 2016. Role of Chondroitin Sulfate (CS) Modification in the Regulation of Protein-tyrosine Phosphatase Receptor Type Z (PTPRZ) Activity: PLEIOTROPHIN-PTPRZ-A SIGNALING IS INVOLVED IN OLIGODENDROCYTE DIFFERENTIATION. *J Biol Chem*. 291:18117-18128.
- Kuboyama, K., N. Tanga, R. Suzuki, A. Fujikawa, and M. Noda. 2017. Protamine neutralizes chondroitin sulfate proteoglycan-mediated inhibition of oligodendrocyte differentiation. *Plos One*. 12:e0189164.
- Lau, L.W., M.B. Keough, S. Haylock-Jacobs, R. Cua, A. Doring, S. Sloka, D.P. Stirling, S. Rivest, and V.W. Yong. 2012. Chondroitin sulfate proteoglycans in demyelinated lesions impair remyelination. *Ann Neurol*. 72:419-432.
- Lee, Y., B.M. Morrison, Y. Li, S. Lengacher, M.H. Farah, P.N. Hoffman, Y. Liu, A. Tsingalia, L. Jin, P.W. Zhang, L. Pellerin, P.J. Magistretti, and J.D. Rothstein. 2012. Oligodendroglia metabolically support axons and contribute to neurodegeneration. *Nature*. 487:443-448.
- Liang, X., N.A. Draghi, and M.D. Resh. 2004. Signaling from integrins to Fyn to Rho family GTPases regulates morphologic differentiation of oligodendrocytes. *J Neurosci*. 24:7140-7149.
- Lodyga, M., X.-h. Bai, A. Kapus, and M.J.J.C.S. Liu. 2010. Adaptor protein XB130 is a Rac-controlled component of lamellipodia that regulates cell motility and invasion. 123:4156-4169.
- Lodyga, M., V. De Falco, X.H. Bai, A. Kapus, R.M. Melillo, M. Santoro, and M. Liu. 2009. XB130, a tissue-specific adaptor protein that couples the RET/PTC oncogenic kinase to PI 3-kinase pathway. *Oncogene*. 28:937-949.
- Lu, Z., L. Ku, Y. Chen, and Y. Feng. 2005. Developmental abnormalities of myelin basic protein expression in fyn knock-out brain reveal a role of Fyn in posttranscriptional regulation. *J Biol Chem*. 280:389-395.
- Maeda, N., H. Hamanaka, A. Oohira, and M. Noda. 1995. Purification, characterization and developmental expression of a brain-specific chondroitin sulfate proteoglycan, 6B4 proteoglycan/phosphacan. *Neuroscience*. 67:23-35.
- Maeda, N., J. He, Y. Yajima, T. Mikami, K. Sugahara, and T. Yabe. 2003. Heterogeneity of the chondroitin sulfate portion of phosphacan/6B4 proteoglycan regulates its binding affinity for pleiotrophin/heparin binding growth-associated molecule. *J Biol Chem*. 278:35805-35811.
- Maeda, N., K. Ichihara-Tanaka, T. Kimura, K. Kadomatsu, T. Muramatsu, and M. Noda. 1999. A receptor-like protein-tyrosine phosphatase PTPzeta/RPTPbeta binds a heparin-binding growth factor midkine. Involvement of arginine 78 of midkine in the high affinity binding to PTPzeta. *J Biol Chem*. 274:12474-12479.

- Maeda, N., T. Nishiwaki, T. Shintani, H. Hamanaka, and M. Noda. 1996. 6B4 proteoglycan/phosphacan, an extracellular variant of receptor-like protein-tyrosine phosphatase zeta/RPTPbeta, binds pleiotrophin/heparin-binding growth-associated molecule (HB-GAM). *J Biol Chem.* 271:21446-21452.
- Maeda, N., and M.J.T.J.o.c.b. Noda. 1998. Involvement of receptor-like protein tyrosine phosphatase ζ/RPTPβ and its ligand pleiotrophin/heparin-binding growth-associated molecule (HB-GAM) in neuronal migration. 142:203-216.
- Mikelis, C., E. Sfaelou, M. Koutsoumpa, N. Kieffer, and E. Papadimitriou. 2009. Integrin alpha(v)beta(3) is a pleiotrophin receptor required for pleiotrophin-induced endothelial cell migration through receptor protein tyrosine phosphatase beta/zeta. *FASEB J.* 23:1459-1469.
- Mitew, S., C.M. Hay, H. Peckham, J. Xiao, M. Koenning, and B. Emery. 2014. Mechanisms regulating the development of oligodendrocytes and central nervous system myelin. *Neuroscience.* 276:29-47.
- Muller, S., P. Kunkel, K. Lamszus, U. Ulbricht, G.A. Lorente, A.M. Nelson, D. von Schack, D.J. Chin, S.C. Lohr, M. Westphal, and T. Melcher. 2003. A role for receptor tyrosine phosphatase zeta in glioma cell migration. *Oncogene.* 22:6661-6668.
- Muramatsu, H., P. Zou, H. Suzuki, Y. Oda, G.-Y. Chen, N. Sakaguchi, S. Sakuma, N. Maeda, M. Noda, and Y. Takada. 2004. α4β1- and α6β1-integrins are functional receptors for midkine, a heparin-binding growth factor. *J Cell Sci.* 117:5405-5415.
- Myers, M.P., J.N. Andersen, A. Cheng, M.L. Tremblay, C.M. Horvath, J.-P. Parisien, A. Salmeen, D. Barford, and N.K.J.J.o.B.C. Tonks. 2001. TYK2 and JAK2 are substrates of protein-tyrosine phosphatase 1B. 276:47771-47774.
- Nandi, S., M. Cioce, Y.G. Yeung, E. Nieves, L. Tesfa, H. Lin, A.W. Hsu, R. Halenbeck, H.Y. Cheng, S. Gokhan, M.F. Mehler, and E.R. Stanley. 2013. Receptor-type protein-tyrosine phosphatase zeta is a functional receptor for interleukin-34. *J Biol Chem.* 288:21972-21986.
- Nave, K.A., and J.L. Salzer. 2006. Axonal regulation of myelination by neuregulin 1. *Curr Opin Neurobiol.* 16:492-500.
- Niisato, K., A. Fujikawa, S. Komai, T. Shintani, E. Watanabe, G. Sakaguchi, G. Katsuura, T. Manabe, and M. Noda. 2005. Age-dependent enhancement of hippocampal long-term potentiation and impairment of spatial learning through the Rho-associated kinase pathway in protein tyrosine phosphatase receptor type Z-deficient mice. *J Neurosci.* 25:1081-1088.
- Nishiwaki, T., N. Maeda, and M. Noda. 1998. Characterization and developmental regulation of proteoglycan-type protein tyrosine phosphatase zeta/RPTPbeta isoforms. *J Biochem.* 123:458-467.
- Niwa, H., K. Yamamura, and J. Miyazaki. 1991. Efficient selection for high-expression transfectants with a novel eukaryotic vector. *Gene.* 108:193-199.
- Papadimitriou, E., E. Pantazaka, P. Castana, T. Tsaliou, A. Polyzos, and D. Beis. 2016. Pleiotrophin and its receptor protein tyrosine phosphatase beta/zeta as regulators of angiogenesis and cancer. *Biochimica et biophysica acta.* 1866:252-265.

- Patel, A.P., I. Tirosh, J.J. Trombetta, A.K. Shalek, S.M. Gillespie, H. Wakimoto, D.P. Cahill, B.V. Nahed, W.T. Curry, R.L. Martuza, D.N. Louis, O. Rozenblatt-Rosen, M.L. Suva, A. Regev, and B.E. Bernstein. 2014. Single-cell RNA-seq highlights intratumoral heterogeneity in primary glioblastoma. *Science*. 344:1396-1401.
- Perez, M.J., N. Fernandez, and J.M. Pasquini. 2013. Oligodendrocyte differentiation and signaling after transferrin internalization: a mechanism of action. *Exp Neurol*. 248:262-274.
- Powers, C., A. Aigner, G.E. Stoica, K. McDonnell, and A. Wellstein. 2002. Pleiotrophin signaling through anaplastic lymphoma kinase is rate-limiting for glioblastoma growth. *J Biol Chem*. 277:14153-14158.
- Ranjan, M., and L.D. Hudson. 1996. Regulation of tyrosine phosphorylation and protein tyrosine phosphatases during oligodendrocyte differentiation. *Mol Cell Neurosci*. 7:404-418.
- Sharma, K., S. Schmitt, C.G. Bergner, S. Tyanova, N. Kannaiyan, N. Manrique-Hoyos, K. Kongi, L. Cantuti, U.K. Hanisch, M.A. Philips, M.J. Rossner, M. Mann, and M. Simons. 2015. Cell type- and brain region-resolved mouse brain proteome. *Nat Neurosci*. 18:1819-1831.
- Shintani, T., and M. Noda. 2008. Protein tyrosine phosphatase receptor type Z dephosphorylates TrkA receptors and attenuates NGF-dependent neurite outgrowth of PC12 cells. *J Biochem*. 144:259-266.
- Shintani, T., E. Watanabe, N. Maeda, and M. Noda. 1998. Neurons as well as astrocytes express proteoglycan-type protein tyrosine phosphatase zeta RPTP beta: analysis of mice in which the PTP zeta/RPTP beta gene was replaced with the LacZ gene. *Neurosci Lett*. 247:135-138.
- Shiozaki, A., M. Lodyga, X.-H. Bai, J. Nadesalingam, T. Oyaizu, D. Winer, S.L. Asa, S. Keshavjee, and M.J.T.A.j.o.p. Liu. 2011. XB130, a novel adaptor protein, promotes thyroid tumor growth. 178:391-401.
- Sim, F.J., J.K. Lang, B. Waldau, N.S. Roy, T.E. Schwartz, W.H. Pilcher, K.J. Chandross, S. Natesan, J.E. Merrill, and S.A. Goldman. 2006. Complementary patterns of gene expression by human oligodendrocyte progenitors and their environment predict determinants of progenitor maintenance and differentiation. *Ann Neurol*. 59:763-779.
- Tamura, H., M. Fukada, A. Fujikawa, and M. Noda. 2006. Protein tyrosine phosphatase receptor type Z is involved in hippocampus-dependent memory formation through dephosphorylation at Y1105 on p190 RhoGAP. *Neurosci Lett*. 399:33-38.
- Tyler, W.A., N. Gangoli, P. Gokina, H.A. Kim, M. Covey, S.W. Levison, and T.L. Wood. 2009. Activation of the mammalian target of rapamycin (mTOR) is essential for oligodendrocyte differentiation. *J Neurosci*. 29:6367-6378.
- Ulbricht, U., M.A. Brockmann, A. Aigner, C. Eckerich, S. Muller, R. Fillbrandt, M. Westphal, and K. Lamszus. 2003. Expression and function of the receptor protein tyrosine phosphatase zeta and its ligand pleiotrophin in human astrocytomas. *J Neuropathol Exp Neurol*. 62:1265-1275.
- Ulbricht, U., C. Eckerich, R. Fillbrandt, M. Westphal, and K. Lamszus. 2006. RNA interference targeting protein tyrosine phosphatase zeta/receptor-type protein tyrosine phosphatase beta suppresses glioblastoma growth in vitro and in vivo. *J Neurochem*. 98:1497-1506.

- Umemori, H., Y. Kadowaki, K. Hirose, Y. Yoshida, K. Hironaka, H. Okano, and T. Yamamoto. 1999. Stimulation of myelin basic protein gene transcription by Fyn tyrosine kinase for myelination. *J Neurosci.* 19:1393-1397.
- Wolf, R.M., J.J. Wilkes, M.V. Chao, and M.D. Resh. 2001. Tyrosine phosphorylation of p190 RhoGAP by Fyn regulates oligodendrocyte differentiation. *J Neurobiol.* 49:62-78.
- Xie, D., F. Shen, S. He, M. Chen, Q. Han, M. Fang, H. Zeng, C. Chen, and Y. Deng. 2016. IL-1beta induces hypomyelination in the periventricular white matter through inhibition of oligodendrocyte progenitor cell maturation via FYN/MEK/ERK signaling pathway in septic neonatal rats. *Glia.* 64:583-602.
- Xu, C., S. Zhu, M. Wu, W. Han, and Y. Yu. 2014. Functional receptors and intracellular signal pathways of midkine (MK) and pleiotrophin (PTN). *Biol Pharm Bull.* 37:511-520.
- Yamanaka, D., T. Akama, T. Fukushima, T. Nedachi, C. Kawasaki, K. Chida, S. Minami, K. Suzuki, F. Hakuno, and S. Takahashi. 2012. Phosphatidylinositol 3-kinase-binding protein, PI3KAP/XB130, is required for cAMP-induced amplification of IGF mitogenic activity in FRTL-5 thyroid cells. *Mol Endocrinol.* 26:1043-1055.
- Yin, G., J. Haendeler, C. Yan, and B.C. Berk. 2004. GIT1 functions as a scaffold for MEK1-extracellular signal-regulated kinase 1 and 2 activation by angiotensin II and epidermal growth factor. *Mol Cell Biol.* 24:875-885.
- Yin, G., Q. Zheng, C. Yan, and B.C. Berk. 2005. GIT1 is a scaffold for ERK1/2 activation in focal adhesions. *J Biol Chem.* 280:27705-27712.
- Yokoyama, K., T. Tezuka, M. Kotani, T. Nakazawa, N. Hoshina, Y. Shimoda, S. Kakuta, K. Sudo, K. Watanabe, Y. Iwakura, and T. Yamamoto. 2011. NYAP: a phosphoprotein family that links PI3K to WAVE1 signalling in neurons. *EMBO J.* 30:4739-4754.
- Yu, M., S.P. Narayanan, F. Wang, E. Morse, W.B. Macklin, and N.S. Peachey. 2011. Visual abnormalities associated with enhanced optic nerve myelination. *Brain Res.* 1374:36-42.

## **Acknowledgements**

I greatly thank my supervisor, Professor Masaharu Noda in the National Institute for Basic Biology (NIBB), for his guidance and suggestions to my research. The opportunity he gave me to work on this research has been an invaluable learning process for me.

I am deeply grateful to Dr. Akihiro Fujikawa for his guidance and suggestions to my research, insightful comments, and instruction of experimental techniques. I would like to thank Drs. K. Kuboyama, R. Suzuki and M. Matsumoto for their help and instruction of experimental techniques. I also thank Drs. Takafumi Shintani, Takeshi Y Hiyama, Hiraki Sakuta, Takashi Matsuda, Kengo Nomura and other members of the Division of Molecular Neurobiology in NIBB for their help and valuable advice. I appreciate N. Nakanishi and Y. Isoshima for their technical assistance and A. Kodama for her secretarial assistance.

I would like to express my gratitude to Professor T. Watanabe in the Graduate School of Humanities and Sciences, Nara Women's University, Japan, for guidance and suggestions to establishing knock-in mice and valuable advice. I would like to thank Drs. H. Kiyonari and T. Abe in the Laboratories for Animal Resource Development and Genetic Engineering, RIKEN Center for Biosystems Dynamics Research, Japan, for guidance and suggestions to establishing knock-in mice. I also thank A. Shiraishi in the Laboratories for Animal Resource Development, RIKEN Center for Biosystems Dynamics Research, Japan, and A. Kishimoto in Nara Women's University, Japan, for help and their technical assistance.

This study was supported by JSPS KAKENHI Grant Numbers: 26830050 and 17K07355, 24500390, 26110722, and 17K07069, 16209008, and the Adaptable & Seamless Technology transfer Program through target-driven R&D (A-STEP). Immunofluorescence photomicrograph images were acquired at the Spectrography and Bioimaging Facility, NIBB Core Research Facilities.

Finally, I would like to give sincere thanks to my dear family for their financial and mental supports. I am grateful to all the people who supported me.